Table 1. Characteristics of the Randomized Cohorts and SVR Rates of Heterozygous Genotype rs12979860CT With Additional Genotyping of rs8099917

Random Sample Size	Sample Number	Mean Age ±SD	Male	HCV RNA ≥400.000 IU/mL	Severe Fibrosis	SVR rs12979680CT/ rs8099917TT	SVR rs12979680CT/ rs8099917TG	P-value
10%	96	47±11	58%	69%	55%	48%	36%	0.408
20%	192	48±11	59%	80%	43%	43%	32%	0.379
30%	295	48±11	60%	72%	48%	50%	38%	0.154
40%	396	47±11	63%	66%	55%	57%	39%	**0.012**
50%	474	47±11	60%	68%	53%	56%	37%	**0.003**
60%	588	48±11	58%	71%	52%	57%	35%	**0.0001**
70%	654	47±11	58%	72%	52%	56%	39%	**0.002**
80%	754	48±11	58%	70%	51%	55%	39%	**0.002**
90%	835	48±11	59%	71%	52%	56%	40%	**0.001**
100%	942	48±11	59%	70%	52%	55%	40%	**0.001**

SD, standard deviation; IU, international units; SVR, sustained virological response; $P < 0.05$ considered to be statistically significant.

fibrosis stage on the SVR rates of genotype rs12979860CT/rs8099917TT and rs12979860CT/rs8099917TG (Supporting Table 1). Again, it becomes obvious that the impact of additional genotyping of rs8099917 on the prediction of SVR is improved in patients with heterozygous genotype of rs12979860 who have high baseline HCV RNA levels ($P = 3.7 \times 10^{-5}$), HCV subtype 1a ($P = 3.3 \times 10^{-5}$), or severe fibrosis stages ($P = 0.001$), being female ($P = 0.023$), or of younger age ($P = 0.029$). Thus, the different patient characteristics most likely explain the differences in the SVR rates.

From that, one possibly may conclude that two SNPs are good in large cohorts but not relevant for clinical practice. However, the idea of large studies is to inform individual clinical practice. Our results derived from a large cohort suggest that algorithms and models that include both rs12979860 and rs809917 as well as baseline parameters and viral factors are informative to guide therapeutic decision making.[3]

Janett Fischer, Ph.D.[1]
Stephan Böhm[1]
Jacob George[2]
Christoph Sarrazin[3]
Thomas Berg, M.D.[1]
[1]*Department of Hepatology, Clinic of Gastroenterology and Rheumatology, Universitätsklinikum Leipzig, Leipzig, Germany*
[2]*Storr Liver Unit, Westmead Hospital and Westmead Millennium Institute, University of Sydney, Sydney, Australia*
[3]*Department of Internal Medicine 1 J. W. Goethe-University Hospital, Frankfurt, Germany*

References

1. Galmozzi E, De Nicola S, Aghema A, Colombo M. Is there a need for more than one IL28B SNP in hepatitis C clinical practice? Hepatology 2013;58;416.
2. Fischer J, Böhm S, Scholz M, Müller T, Witt H, George J, et al. Combined effects of different interleukin-28B gene variants on the outcome of dual combination therapy in chronic hepatitis C virus type 1 infection. Hepatology 2012;55:1700-1710.
3. Ladero JM, Martin EG, Fernández C, Carballo M, Devesa MJ, Martínez C, et al. Predicting response to therapy in chronic hepatitis C: an approach combining interleukin-28B gene polymorphisms and clinical data. J Gastroenterol Hepatol 2012;27:279-285.

DOI 10.1002/hep.25923
Supported by the German Competence Network for Viral Hepatitis (Hep-Net), funded by the German Ministry of Education and Research (BMBF, Grant No. 01 KI 0437, Project No. 10.1.3 and Core Project No. 10.1 Genetic host factors in viral hepatitis and Genetic Epidemiology Group in viral hepatitis), by the EU-Vigilance network of excellence combating viral resistance (VIRGIL, Project No. LSHM-CT-2004-503359), and by the BMBF Project: Host and viral determinants for susceptibility and resistance to hepatitis C virus infection (Grant No. 01KI0787). Parts of the work were supported by an Australian Research Council Linkage Project Grant (LP00990067), a National Health and Medical Research Council Grant (1006759) and the Robert W. Storr Bequest to the Sydney Medical Foundation, University of Sydney.

Plasma Lysophosphatidic Acid Levels and Hepatocellular Carcinoma

To the Editor:

We read with interest the article by Mazzocca et al.,[1] showing that serum lysophosphatidic acid (LPA) levels are increased in hepatocellular carcinoma (HCC) patients correlated with tumor burden, while not enhanced in cirrhosis patients. However, we think that their LPA values in serum samples need to be carefully evaluated, because of some technical issues in the measurement of LPA levels in blood samples. First, because LPA is released from platelets, LPA has been measured in plasma but not in serum when evaluating its clinical significance.[2,3] Second, as we previously demonstrated,[4] LPA levels in plasma samples are markedly increased after sample preparation unless the temperature is kept under strict control, potentially because the synthetic enzyme autotaxin (ATX) and the substrate lysophosphatidyl choline coexist in plasma samples to abundantly produce LPA. LPA was once reported as a biomarker of ovarian cancer,[2] but contrary data were later demonstrated, in which a distinct sampling of plasma may explain this discrepancy.[3] Indeed, LPA levels in serum reported by Mazzocca et al. were approximately 10 times higher than the previously reported LPA levels in plasma.[2,3] If their LPA values in serum were increased after sampling similarly in each sample, plasma LPA levels might be correlated with HCC burden as reported. To clarify this, we have newly measured plasma LPA levels in HCC patients,

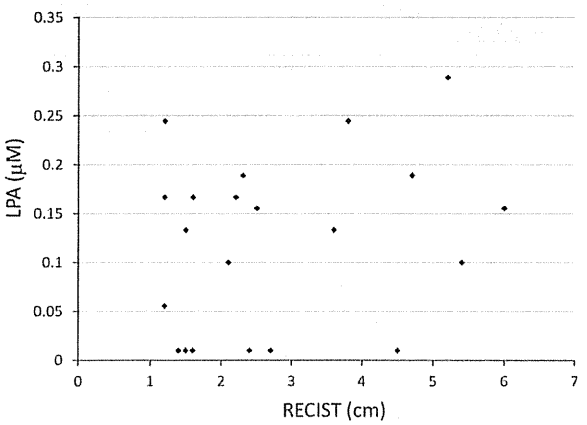

Fig. 1. Plasma LPA levels and HCC burden. Plasma LPA levels, measured in 21 HCC patients (13 males and 8 females; 2 patients with chronic hepatitis B, 15 with chronic hepatitis C, and 4 with non-B non-C chronic liver disease), were not significantly correlated with HCC burden as evaluated by RECIST (Response Evaluation Criteria in Solid Tumors; Spearman rank, $r = 0.158$, $P = 0.4937$). This study was approved by the Institutional Research Ethics Committee and informed consent was obtained for the use of the samples.

and found that they were not correlated with tumor burden, as shown in Fig. 1. Moreover, plasma LPA levels in HCC patients (0.12 ± 0.09 mM, mean $\pm$ SD, n = 21), were not different from the previously reported levels in non-HCC patients with chronic hepatitis C (0.10 ± 0.05 mM).[5] Although Mazzocca et al. reported no enhancement of serum LPA levels in cirrhosis patients, we[5] and others[6] previously showed that plasma LPA levels and serum ATX activity were increased in chronic liver diseases in association with fibrosis and cholestatic pruritus, from which HCC frequently arises. Collectively, a role of LPA in HCC should be cautiously analyzed.

Hitoshi Ikeda, M.D., Ph.D.[1,2]
Kenichiro Enooku, M.D. Ph.D.[1,2]
Ryunosuke Ohkawa, Ph.D.[1]
Kazuhiko Koike, M.D., Ph.D.[2]
Yutaka Yatomi, M.D., Ph.D.[1]
[1]*Department of Clinical Laboratory Medicine*
Graduate School of Medicine
University of Tokyo
Tokyo, Japan
[2]*Department of Gastroenterology*
Graduate School of Medicine
University of Tokyo
Tokyo, Japan

References

1. Mazzocca A, Dituri F, Lupo L, Quaranta M, Antonaci S, Giannelli G. Tumor-secreted lysophostatidic acid accelerates hepatocellular carcinoma progression by promoting differentiation of peritumoral fibroblasts in myofibroblasts. Hepatology 2011;54:920-930.
2. Xu Y, Shen Z, Wiper DW, Wu M, Morton RE, Elson P, et al. Lysophosphatidic acid as a potential biomarker for ovarian and other gynecologic cancers. JAMA 1998;280:719-723.
3. Baker DL, Morrison P, Miller B, Riely CA, Tolley B, Westermann AM, et al. Plasma lysophosphatidic acid concentration and ovarian cancer. JAMA 2002;287:3081-3082.
4. Nakamura K, Ohkawa R, Okubo S, Tozuka M, Okada M, Aoki S, et al. Measurement of lysophospholipase D/autotaxin activity in human serum samples. Clin Biochem 2007;40:274-277.
5. Watanabe N, Ikeda H, Nakamura K, Ohkawa R, Kume Y, Aoki J, et al. Both plasma lysophosphatidic acid and serum autotaxin levels are increased in chronic hepatitis C. J Clin Gastroenterol 2007;41:616-623.
6. Kremer AE, Martens JJ, Kulik W, Rueff F, Kuiper EM, van Buuren HR, et al. Lysophosphatidic acid is a potential mediator of cholestatic pruritus. Gastroenterology 2010;139:1008-1018.

DOI 10.1002/hep.25886
Potential conflict of interest: Nothing to report.

Reply:

Ikeda et al. remark that platelets are a main source of lysophosphatidic acid (LPA) and therefore the interpretation of LPA serum concentrations deserves careful attention. However, the same authors previously reported[1] an inverse correlation between plasma LPA concentrations and the number of platelets in patients with chronic C hepatitis. Therefore, it is possible that in physiologic conditions platelets remain the main source of LPA, while in chronic inflammation such as hepatitis C, liver cirrhosis, or hepatocellular carcinoma (HCC), the platelet contribution to LPA production may likely become less relevant. In our study we analyzed sera for LPA detection in healthy donors, liver cirrhosis, and HCC patients, performing well-standardized procedures of collection for each sample. Thus, the contribution of platelets to the LPA concentration was, in reality, normalized. On the contrary, the authors should consider that even in plasma or whole blood, platelet activation is an extremely difficult problem to deal with and control. For example, prolonged tourniquet application, or twisting of the needle in the vein, are major factors interfering with the function of platelets during blood withdrawal, as reviewed by Ruggeri.[2] Unfortunately, these limitations are common for a number of molecules involved both in cancer and in blood cell biology.[3]

Moreover, Ikeda et al. investigated patients with chronic hepatitis C, in whom the inflammatory response is a key component of the tissue microenvironment. In their study, the fibrotic status was also questionable, due to their choice of statistical method (comparison among groups should be done with Kruskal-Wallis tests), and because of the very limited number of patients (14), further stratified into four different groups, which means the conclusions were affected by low power.[1] In our study,[4] we compared liver cirrhosis versus HCC. In the former case, the inflammation is reduced while the fibrotic response is increased, consequently inducing a different microenvironment response.[5] This could explain why patients with liver cirrhosis display relatively low levels of LPA. In addition, it is conceivable that when HCC develops in cirrhotic liver, LPA levels rise once more, as in cases of active inflammatory states (i.e., viral hepatitis). Another key point is patient selection. Ikeda et al. do not provide any information with regard to the clinical features of the patients, i.e., etiology, BCLC stage, previous therapy, etc., as well as how they calculated the size of the tumor in patients with multifocal disease, for instance. Finally, some differences between Caucasian and Asian patients with HCC are to be expected, since the natural history is completely different in Western and Southeast Asian countries.[6] In our study,[4] we demonstrated that LPA has a role in promoting tumor progression and we did not attempt to speculate about the use of LPA as a clinical biomarker. To validate LPA as a potential biomarker for HCC a different study design is required, as well as first considering the power of the study. The enhancement of serum LPA levels reported by Watanabe et al.[1] referred to a relatively small number of patients with chronic hepatitis C. In addition, the

HEPATOLOGY
Official Journal of the American Association for the Study of Liver Diseases

MicroRNA-140 Acts as a Liver Tumor Suppressor by Controlling NF-κB Activity by Directly Targeting DNa Methyltransferase 1 (Dnmt1) Expression

Akemi Takata,[1] Motoyuki Otsuka,[1] Takeshi Yoshikawa,[1] Takahiro Kishikawa,[1] Yohko Hikiba,[2] Shuntaro Obi,[3] Tadashi Goto,[1] Young Jun Kang,[4] Shin Maeda,[1] Haruhiko Yoshida,[1] Masao Omata,[1] Hiroshi Asahara,[5,6,7] and Kazuhiko Koike[1]

MicroRNAs (miRNAs) are small RNAs that regulate the expression of specific target genes. While deregulated miRNA expression levels have been detected in many tumors, whether miRNA functional impairment is also involved in carcinogenesis remains unknown. We investigated whether deregulation of miRNA machinery components and subsequent functional impairment of miRNAs are involved in hepatocarcinogenesis. Among miRNA-containing ribonucleoprotein complex components, reduced expression of DDX20 was frequently observed in human hepatocellular carcinomas, in which enhanced nuclear factor-κB (NF-κB) activity is believed to be closely linked to carcinogenesis. Because DDX20 normally suppresses NF-κB activity by preferentially regulating the function of the NF-κB-suppressing miRNA-140, we hypothesized that impairment of miRNA-140 function may be involved in hepatocarcinogenesis. DNA methyltransferase 1 (Dnmt1) was identified as a direct target of miRNA-140, and increased Dnmt1 expression in DDX20-deficient cells hypermethylated the promoters of metallothionein genes, resulting in decreased metallothionein expression leading to enhanced NF-κB activity. MiRNA-140-knockout mice were prone to hepatocarcinogenesis and had a phenotype similar to that of DDX20 deficiency, suggesting that miRNA-140 plays a central role in DDX20 deficiency-related pathogenesis. ***Conclusion*****: These results indicate that miRNA-140 acts as a liver tumor suppressor, and that impairment of miRNA-140 function due to a deficiency of DDX20, a miRNA machinery component, could lead to hepatocarcinogenesis. (HEPATOLOGY 2013;57:162-170)**

Hepatocellular carcinoma (HCC) is the third most common cause of cancer-related mortality worldwide.[1] Although multiple major risk factors have been identified, such as infection with hepatitis viruses B or C, the molecular mechanisms underlying HCC development remain poorly understood, hindering the development of novel therapeutic approaches. Therefore, a better understanding of the molecular pathways involved in hepatocarcinogenesis is critical for the development of new therapeutic options.

Nuclear factor-κB (NF-κB) is one of the best-characterized intracellular signaling pathways. Its activation is a common feature of human HCC.[2-4] It acts as an inhibitor of apoptosis and as a tumor promoter[4,5] and is associated with the acquisition of a transformed phenotype during hepatocarcinogenesis.[6] In fact, studies using patient samples suggest that NF-κB activation in the liver leads to the development of HCC.[7] Although there are conflicting reports,[8] activation of the NF-κB pathway in the liver is crucial for the initiation and promotion of HCC.[4]

Abbreviations: DEN, diethylnitrosamine; Dnmt1, DNA methyltransferase 1; HCC, hepatocellular carcinoma; miRNA; microRNA; miRNP, miRNA-containing ribonucleoprotein; MT, metallothionein; NF-κB, nuclear factor-κB; RT-PCR, reverse-transcription polymerase chain reaction; TNF-α, tumor necrosis factor-α; TRAIL, TNF-related apoptosis-inducing ligand; UTR, untranslated region.

From the [1]Department of Gastroenterology, Graduate School of Medicine, The University of Tokyo, Tokyo, Japan; the [2]Division of Gastroenterology, Institute for Adult Diseases, Asahi Life Foundation, Tokyo, Japan; the [3]Department of Hepatology, Kyoundo Hospital, Tokyo, Japan; the [4]Department of Immunology and Microbial Science, and the [5]Department of Molecular and Experimental Medicine, The Scripps Research Institute, La Jolla, CA; the [6]Department of Systems BioMedicine, Tokyo Medical and Dental University, Tokyo, Japan; and [7]CREST, Japan Science and Technology Agency, Tokyo, Japan.

Received March 30, 2012; accepted July 18, 2012.

Supported by Grants-in-Aid from the Ministry of Education, Culture, Sports, Science and Technology, Japan (#22390058, #23590960, and #20390204) (M. O., T. G., and K. K.); Health Sciences Research Grants from the Ministry of Health, Labor and Welfare of Japan (Research on Hepatitis) (to K. K.); National Institutes of Health Grant R01AI088229 (to Y. J. K.); the Miyakawa Memorial Research Foundation (to A. T.); and grants from the Sagawa Foundation for Promotion of Cancer Research, the Astellas Foundation for Research on Metabolic Disorders, and the Cell Science Research Foundation (to M. O.).

MicroRNAs (miRNAs) are small RNA molecules that regulate the expression of target genes and are involved in various biological functions.[9-12] Although specific miRNAs can function as either suppressors or oncogenes in tumor development, a general reduction in miRNA expression is commonly observed in human cancers.[13-22] In this context, it can be hypothesized that deregulation of the machinery components involved in miRNA function may be related to the functional impairment of miRNAs and the pathogenesis of carcinogenesis.

In this study, we show that the expression of DDX20, an miRNA-containing ribonucleoprotein (miRNP) component, is frequently decreased in human HCC. Because DDX20 is required for both the preferential loading of miRNA-140 into the RNA-induced silencing complex and its function,[23] we hypothesized that DDX20 deficiency would lead to hepatocarcinogenesis via impaired miRNA-140 function. MiRNA-140 knockout mice were indeed more prone to hepatocarcinogenesis, and we identified a possible molecular pathway from DDX20 deficiency to liver cancer.

Materials and Methods

Mouse and Liver Tumor Induction. MiRNA-140$^{-/-}$ mice have been described.[24] Recombinant murine tumor necrosis factor-α (TNF-α) (25 μg/kg; Wako, Osaka, Japan) was injected into the tail vein, and the mice were sacrificed 1 hour later. To induce liver tumors, 15-day-old mice received an intraperitoneal injection of diethylnitrosamine (DEN) (25 mg/kg body weight), and were sacrificed 32 weeks later. All animal experiments were performed in compliance with the regulations of the Animal Use Committee of the University of Tokyo and the Institute for Adult Disease, Asahi Life Foundation.

Plasmids. FLAG-tagged human DDX20-expressing plasmids were as described.[23] The pGL3-based reporter plasmid containing Dnmt1 3′ untranslated region (UTR) sequences was provided by G. Marucucci.[25]

Detailed Materials and Methods. The detailed experimental procedures of clinical samples, cells, plasmids, reporter assays, reverse-transcription polymerase chain reaction (RT-PCR) analysis, antibodies, western blotting, cell assays, immunohistochemistry, microarray analysis, methylation analysis, and electrophoretic mobility-shift assay are described in the Supporting Information.

Statistical Analysis. Statistically significant differences between groups were determined using a Wilcoxon rank-sum test. A Wilcoxon signed-rank test was used for statistical comparisons of protein expression levels between HCC and surrounding noncancerous tissues.

Table 1. Cases with Differential Expression Levels of miRNP Components in HCC (n = 10)

Gene ID	Gene Symbol	Decreased	Increased	No Change
23405	Dicer1	2	1	7
27161	EIF2C2 (AGO2)	1	1	8
6895	TARBP2(TRBP2)	2	0	8
11218	DDX20 (GEMIN3)	8	0	2
50628	GEMIN4	1	0	9

The expression levels of each miRNP component were determined via immunohistochemistry.

The numbers indicate the number of cases that had the differential expression levels (decreased, increased, or no change) in HCC tissues compared with those in surrounding liver tissues.

Results

DDX20 Expression Is Frequently Decreased in HCC. The expression levels of proteins reported to be miRNP components (Dicer, Ago2, TRBP2, DDX20 [also known as Gemin3], and Gemin4)[26] were initially determined via immunohistochemistry in HCC and noncancerous background liver tissues from 10 patients. DDX20 expression was lower in HCC tissue compared with the surrounding noncancerous tissue in 8 of 10 cases, whereas expression of the other genes was unchanged (Table 1 and Supporting Fig. 1). Therefore, and because DDX20 was recently identified as a possible liver tumor suppressor in mice,[27] we determined its role as a human HCC suppressor.

DDX20 protein expression was lower in several HCC cell lines, such as Huh7 and Hep3B (Fig. 1A), compared with normal hepatocytes. DDX20 protein levels were also lower in human HCC needle biopsy specimens than in surrounding noncancerous liver tissue (Fig. 1B). Immunohistochemical analysis

Address reprint requests to: Motoyuki Otsuka, M.D., Department of Gastroenterology, Graduate School of Medicine, University of Tokyo, 7-3-1 Hongo, Bunkyo-ku, Tokyo 113-8655, Japan. E-mail: otsukamo-tky@umin.ac.jp; fax: (81)-3-3814-0021.

View this article online at wileyonlinelibrary.com.

DOI 10.1002/hep.26011

Potential conflict of interest: Nothing to report.

Additional Supporting Information may be found in the online version of this article.

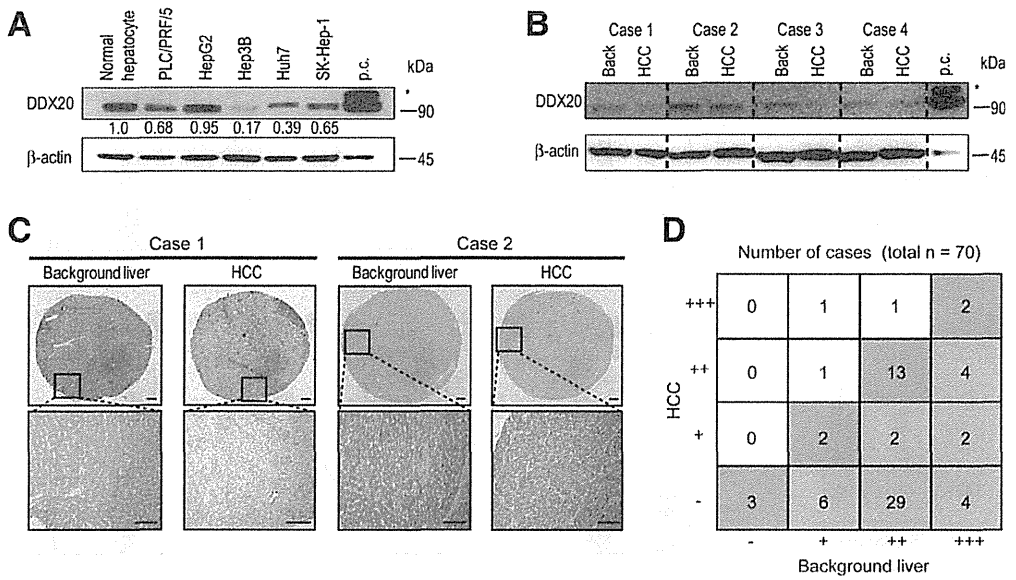

Fig. 1. Reduced DDX20 expression levels in hepatocellular carcinoma. (A) DDX20 protein expression in HCC cell lines. Numbers between the panels indicate DDX20 protein levels normalized to β-actin levels. Lysates of 293T cells transiently transfected with a FLAG-tagged DDX20-expressing plasmid yielded two DDX20 bands corresponding to the endogenous DDX20 protein and the transfected FLAG-tagged DDX20 protein (*) as a positive control (p.c.; far right lane). Data represent the results of three independent determinations. (B) DDX20 protein expression in four HCC needle biopsy specimens and in the surrounding noncancerous background liver tissue (Back). *Positive control. (C) Immunohistochemical analysis of DDX20 protein expression in HCC and surrounding tissues (background liver). Two representative cases are shown. Scale bars, 500 μm. The lower panels display magnified images of the boxed areas in the upper panels. (D) Grid summarizing DDX20 immunohistochemical staining data from 70 cases. In 47 cases (pink shading), DDX20 protein levels were lower in the HCC tissues than in the surrounding tissues ($P < 0.05$; Wilcoxon signed-rank test).

confirmed that DDX20 expression was frequently lower in HCC than in surrounding noncancerous liver tissue (Fig. 1C,D). Specifically, 47 of 70 cases examined showed reduced DDX20 protein expression in HCC versus background noncancerous liver tissue (Fig. 1D and Supporting Table 1). These results indicate that the expression of DDX20, an miRNP component, is frequently reduced in human HCC, and suggest that this reduced DDX20 expression might be involved in the pathogenesis of a subset of HCC cases.

NF-κB Activity Is Enhanced by DDX20 Deficiency. Because DDX20 knockout mice are embryonic-lethal,[28] DDX20 has been suggested to have important biological roles. DDX20, a DEAD-box protein,[29] was originally found to interact with survival motor neuron protein.[30] Later, it was identified as a major component of miRNPs,[31] which may mediate miRNA function. As we have reported, DDX20 is preferentially involved in miRNA-140-3p function,[23] acting as a suppressor of NF-κB activity in the liver.[32] DDX20-knockdown PLC/PRF/5 cells exhibit enhanced NF-κB activity[23] (Fig. 2A). Whereas the proliferation rates of DDX20-knockdown cells and control cells were comparable (Fig. 2B), apoptotic cell death after stimulation with TNF-related apoptosis-inducing ligand (TRAIL), which induces both cell apoptosis and NF-κB activation,[33] was significantly reduced in DDX20-knockdown cells (Fig. 2C). Similar results were obtained using DDX20-knockdown HepG2 cells (Supporting Fig. 2A-D). Conversely, NF-κB activity was reduced, but cell proliferation remained unchanged, in Hep3B cells stably overexpressing DDX20 (Fig. 2D,E). Sensitivity to TRAIL-induced apoptosis was restored in these cells (Fig. 2F). Similar results were also obtained using Huh7 cells (Supporting Fig. 2E-H). These data confirm a previous report that DDX20 deficiency enhances NF-κB activity and the downstream events of this pathway.

Metallothionein Expression Is Decreased by DDX20 Deficiency. Next, to investigate the biological consequences of DDX20 deficiency, we examined the changes in transcript levels in DDX20-knockdown cells using microarrays (GEO accession number: GSE28088). The expression of genes driven by NF-κB that are related to carcinogenesis, such as FASLG, IRAK1, CARD9, and Galectin-1, were enhanced significantly in DDX20-knockdown cells, as expected (Table 2). To determine the mechanism underlying the enhanced NF-κB activation in DDX20-deficient cells, we searched for candidate genes and noticed that the

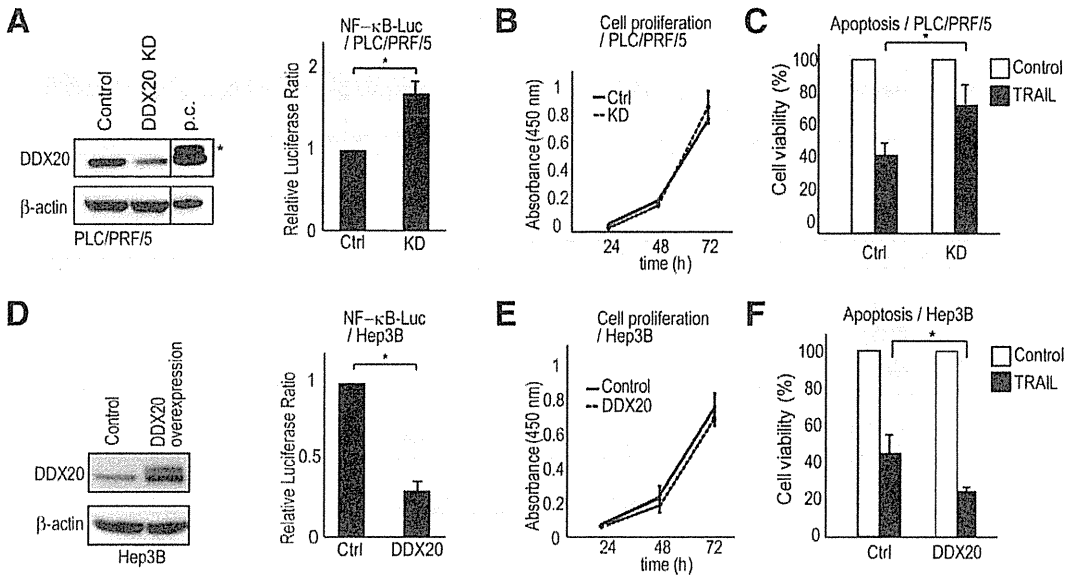

Fig. 2. Modulation of downstream events of the nuclear factor-κB pathway by DDX20. (A) Left: Establishment of stable DDX20-knockdown (DDX20 KD) PLC/PRF/5 cells. *Positive control (p.c.). Right: DDX20 deficiency enhances TNF-α–induced NF-κB activity. NF-κB reporter plasmids were transiently transfected into control (Ctrl) or DDX20-knockdown (KD) PLC/PRF/5 cells. The cells were then treated with TNF-α (5 ng/mL) or vehicle for 6 hours. *$P < 0.05$. Data are presented as the mean ± SD of three independent determinations. (B) Cell proliferation rates were comparable for control (Ctrl) and DDX20-knockdown (KD) PLC/PRF/5 cells. Data are presented as the mean ± SD of three determinations. (C) DDX20 deficiency reduces TRAIL-induced apoptotic cell death. Control (Ctrl) and DDX20-knockdown (KD) PLC/PRF/5 cells were incubated with 25 ng/mL TRAIL. Data represent cell viability after TRAIL stimulation (gray bars) relative to the number of vehicle-treated cells (white bars). *$P < 0.05$. Data are presented as the mean ± SD of triplicate determinations. (D) Left: Establishment of stable DDX20-overexpressing cells. Hep3B cells were infected with control or FLAG-tagged DDX20-overexpressing lentiviruses and selected on puromycin. Western blot analysis confirmed increased expression of DDX20 protein. Right: DDX20 overexpression suppresses TNF-α–induced NF-κB activity. NF-κB reporter plasmids were transiently transfected into Hep3B control (Ctrl) and DDX20-overexpressing (DDX20) cells treated with TNF-α for 6 hours. Data are presented as the mean ± SD of three independent determinations. *$P < 0.05$. (E) Proliferation of control (Ctrl) and DDX20-overexpressing (DDX20) Hep3B cells was measured as described in (B). (F) DDX20 overexpression reduces TRAIL-induced apoptotic cell death. Data for control (Ctrl) and DDX20-overexpressing (DDX20) Hep3B cells are shown. *$P < 0.05$.

Table 2. Increased Expression of NF-κB–Related Genes in DDX20-Knockdown HepG2 Cells Compared with Wild-Type Cells

RefSeq ID	Symbol	Description	Ratio	Representative Gene Function
NM_000639	FASLG	Fas ligand	3.5	NF-κB target, apoptosis
NM_052813	C9orf151	CARD9	2.5	NF-κB cascade, NF-κB target
NM_014959	CARD8	Tumor up-regulated CARD-containing antagonist of CASP9 (TUCAN)	2.2	NF-κB target
NM_131917	FAF1	FAS-associated factor 1 (hFAF1)	1.9	Cytoplasmic sequestering of NF-κB, NF-κB target
NM_020644	TMEM9B	Transmembrane protein 9B precursor	1.9	Positive regulation of NF-κB transcription factor activity
NM_017544	NKRF	ITBA4 protein	1.9	Negative regulation of transcription
NM_006247	PPP5C	Protein phosphatase T	1.8	Positive regulation of NF-κB cascade
NM_020345	NKIRAS1	KappaB-Ras1	1.8	NF-κB cascade
NM_001569	IRAK1	IRAK-1	1.7	Positive regulation of NF-κB transcription factor activity
NM_177951	PPM1A	Protein phosphatase 1A	1.7	Positive regulation of NF-κB cascade
NM_018098	ECT2	Epithelial cell-transforming sequence 2 oncogene	1.6	Positive regulation of NF-κB cascade
NM_002305	LGALS1	Galectin-1 (putative MAPK-activating protein MP12)	1.6	Positive regulation of NF-κB cascade
NM_015093	TAB2	TAK1-binding protein 2	1.6	Positive regulation of NF-κB cascade
NM_004180	TANK	TRAF-interacting protein	1.5	NF-κB cascade
NM_014976	PDCD11	Programmed cell death protein 11	1.5	rRNA processing
NM_015336	ZDHHC17	Putative NF-κB-activating protein 205	1.5	Positive regulation of NF-κB cascade
NM_002503	NFKBIB	IKB-β	1.5	Cytoplasmic sequestering of NF-κB
NM_138330	ZNF675	Zinc finger protein 675	1.5	Negative regulation of NF-κB transcription factor activity

The genes were identified as NF-κB–related based on the Gene Ontology and the GeneCodis Databases.

Table 3. Decreased Expression Levels of MT Genes in DDX20 Knockdown HepG2 Cells Compared with Wild-Type Cells

Symbol	Description	Ratio
MT1E	Metallothionein-1E	**0.12**
MT1F	Metallothionein-1F	**0.36**
MT1H	Metallothionein-1H	**0.16**
MT1G	Metallothionein-1G	**0.06**
MT1M	Metallothionein-1M	**0.24**
MT1X	Metallothionein-1X	**0.27**
MT2A	Metallothionein-2	**0.28**
MT3	Metallothionein-3	0.84
MTL5	Metallothionein-like 5 (Tesmin)	1.12

Numbers in boldface type indicate values <0.5.

expression levels of a group of metallothioneins (MTs), such as MT1E, MT1F, MT1G, MT1M, MT1X, and MT2A, were all significantly decreased when DDX20 was deficient (Table 3). The decreased expression of MTs in DDX20-knockdown HepG2 and PLC/PRF/5 cells was confirmed via quantitative RT-PCR (Fig. 3a and Supporting Fig. 3). Expression of MT-3, which was not altered in the microarray analysis, was similarly unaltered in quantitative RT-PCR analysis. Notably, it was already known that MTs are frequently silenced in human primary liver cancers.[34-36] In addition, MT knockout mice have enhanced NF-κB activity, likely due to reactive oxygen species, and these mice are more prone to hepatocarcinogenesis.[37] These results suggest that DDX20 deficiency enhances NF-κB activity by decreasing the expression of MTs, which could facilitate the development of liver cancer.

MiRNA-140 Directly Targets Dnmt1. Because MT expression is regulated principally by CpG island methylation in their promoter regions,[38,39] we examined the quantitative methylation status of MT promoters in DDX20-knockdown cells. The CpG islands of the MT1E, MT1G, MT1M, MT1X, and MT2A promoters, and the CpG shores of the MT1F promoters, were significantly more highly methylated under DDX20-deficient conditions, as determined by the comprehensive Illumina Quantitative Methylation BeadChip method (Table 4, Supporting Table 2, and GSE 37633). A crucial step in DNA methylation involves DNA methyltransferase (Dnmt), which catalyzes the methylation of CpG dinucleotides in genomic DNA.[40] The methylation status of MT promoters is mediated specifically by Dnmt1.[41] Because Dnmt1 contains a predicted miRNA-140-3p target site in its 3′ UTR, with a perfect match to its seed sequences (Fig. 3B), and because the effects of miRNA-140-3p activity were impaired in DDX20-knockdown cells,[23] it was hypothesized that whereas miRNA-140 normally targets and suppresses Dnmt1 protein expression, miRNA-140-3p dysfunction due to DDX20 deficiency results in enhanced Dnmt1 expression, leading to hypermethylation of MT promoters. Consistent with this hypothesis, Dnmt1 expression was increased significantly in DDX20-knockdown cells (Fig. 3C). miRNA-140 precursor overexpression suppressed activity of the Dnmt1 3′ UTR reporter construct, the effect of which was lost when two mutations were introduced into its seed sequences (Fig. 3D). MiRNA-140 precursor overexpression suppressed Dnmt1 protein expression (Fig. 3E). These results indicate that miRNA-140 directly targets Dnmt1 and suppresses its expression in the normal state. Consistently, decreased DDX20, increased Dnmt1, and decreased MT expression were detected together in human clinical HCC samples, as determined via immunohistochemistry (Fig. 3F). By contrast, miRNA-140 precursor-overexpressing Huh7 cells showed increased expression of MTs and reduced NF-κB activity *in vitro* (Supporting Fig. 4A,B). Moreover, the increase in the number of spheres formed from PLC/PRF/5 cells due to DDX20 knockdown was antagonized by treatment with an NF-κB inhibitor or a demethylating agent (Supporting Fig. 5). Taken together, these results suggest that the up-regulated Dnmt1 protein expression caused by functional impairment of miRNA-140-3p due to DDX20 deficiency results in decreased expression of MTs *via* enhanced methylation at the CpG sites in their promoters. This may lead to enhanced NF-κB activity and cellular transformation at least *in vitro*.

MiRNA-140 Is a Liver Tumor Suppressor. To further examine the biological consequences of functional impairment of miRNA-140 due to DDX20 deficiency, we determined the phenotypes of miRNA-140 knockout (miRNA-140$^{-/-}$) mice (Fig. 4A). Similar to the *in vitro* DDX20 knockdown results, Dnmt1 expression was increased and MT levels decreased in the liver tissue of these mice (Fig. 4B). NF-κB–DNA binding activity was enhanced in the livers of miRNA-140$^{-/-}$ mice after tail-vein injection of TNF-α, a crucial cytokine that induces NF-κB activity and hepatocarcinogenesis (Fig. 4C). As was found in MT knockout mice, phosphorylation of p65 at serine 276, which is critical for p65 activation, was significantly increased in the livers of miRNA-140$^{-/-}$ mice after DEN exposure, which induces NF-κB activation and liver tumors[37] (Fig. 4D). Notably, the size and number of liver tumors that developed 8 months after DEN exposure were markedly elevated in miRNA-140$^{-/-}$ mice compared with control mice (Fig. 4E,F). These results indicate that miRNA-140$^{-/-}$ mice are indeed

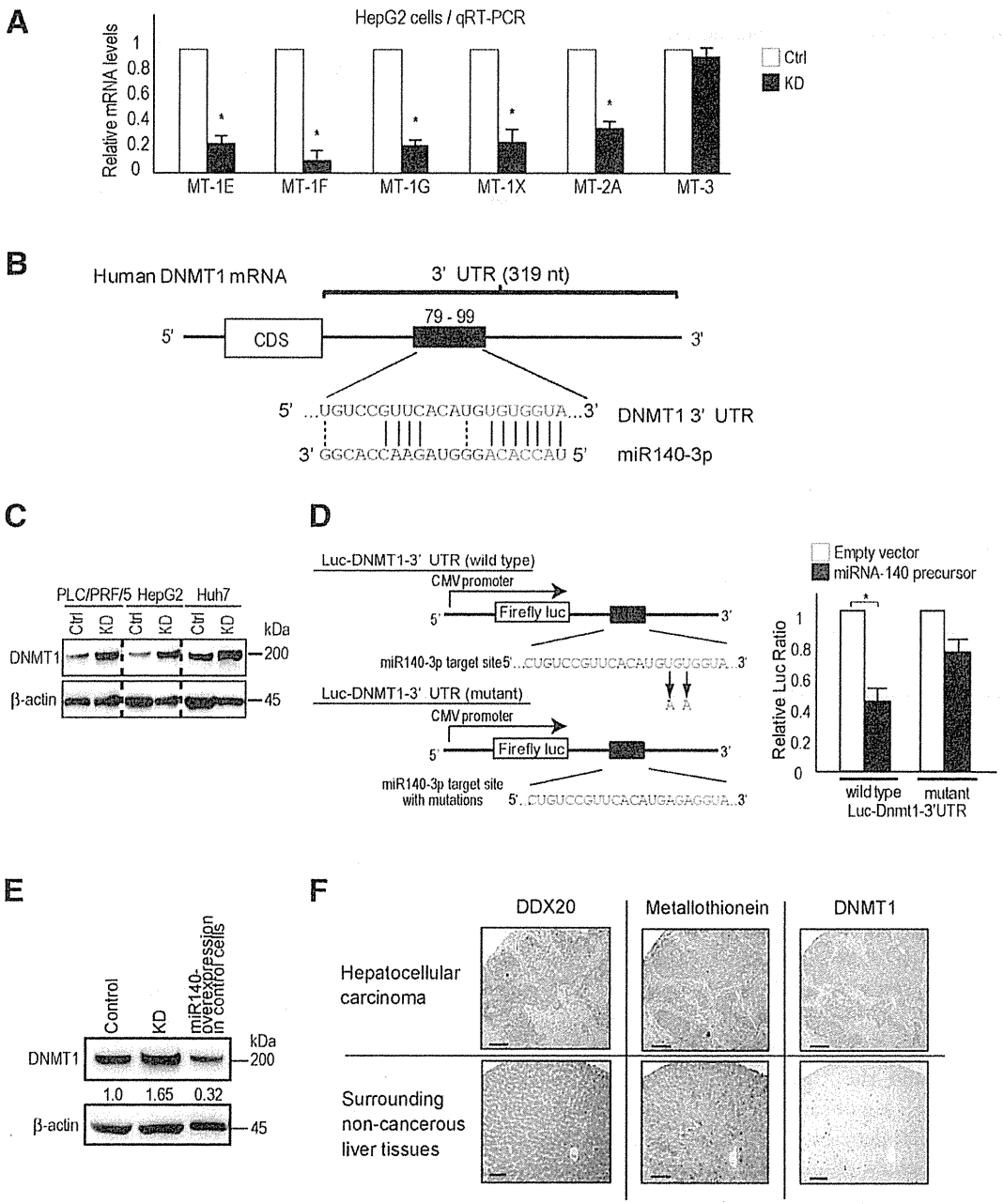

Fig. 3. Targeting of Dnmt1 by miRNA-140-3p and reduced MT expression. (A) The expression levels of MTs were determined using quantitative reverse-transcriptase polymerase chain reaction. The relative expression ratios of the MTs in control (white bars) and DDX20-knockdown (black bars) HepG2 cells were calculated by normalizing control cell values to 1.0. The data represent the mean ± SD of three independent determinations. $^*P < 0.05$. (B) Putative miRNA-140-3p target sites in the 3′ UTR of human Dnmt1. Seed sequences are indicated in red. (C) Dnmt1 expression was increased in DDX20-knockdown cells. Ctrl, control cells; KD, DDX20-knockdown cells. (D) Left: Schematic diagrams of wild-type (upper) and mutant (lower) luciferase reporter constructs (Luc-Dnmt1-3′ UTRs) carrying the Dnmt1 3′ UTR region harboring the putative miRNA-140-3p target site. The mutant seed sequence contained two nucleotide substitutions. Right: The Dnmt1 3′ UTR is targeted directly by miRNA-140-3p. Cells were cotransfected with Luc-Dnmt1-3′ UTR (wild-type or mutant) plus either an empty vector (white bars) or a plasmid expressing the miRNA-140 precursor (black bars). Data are the mean ± SD of three independent determinations. (E) Overexpression of miRNA-140 reduces Dnmt1 expression in control cells. Values between the panels indicate Dnmt1 protein levels normalized to those of β-actin. KD, DDX20 knockdown cells. (F) Representative histochemical images showing expression of DDX20, Dnmt1, and MT proteins in HCC (upper three panels) and surrounding tissue (lower panels). Compared with adjacent noncancerous liver tissue, HCCs exhibited decreased DDX20 and MT expression and increased Dnmt1 expression. Note that adjacent sections were stained for each protein. Scale bar, 50 μm.

Table 4. Methylation Levels in CpG Islands of the MT Genes in DDX20-Knockdown HepG2 Cells Compared with Control Cells

Symbol	CpG Island Methylation Ratio	Target ID
MT1E	**1.14**	cg00178359
	1.29	cg06463589
	3.65	cg02512505
	1.02	cg15134649
MT1G	**2.14**	cg16452857
	1.03	cg27367960
	1.00	cg03566142
	0.99	cg07791866
MT1M	**1.16**	cg02132560
	0.98	cg02160530
	1.03	cg04994964
MT1X	**1.24**	cg05596720
	1.05	cg26802333
	1.06	cg09147880
	1.01	cg08872713
MT2A	**2.06**	cg07395075
	0.94	cg20430434

Values were determined using the quantitative Illumina Human Methylation BeadsChip. Boldface values indicate increased methylation levels in DDX20 knockdown cells.

more prone to liver cancer development and suggest that miRNA-140 acts as a liver tumor suppressor, probably by suppressing NF-κB activity, although we cannot completely exclude other molecular mechanisms. Nonetheless, these results also suggest that the impairment of miRNA-140 function due to DDX20 deficiency may lead to hepatocarcinogenesis in humans, as we have observed in miRNA-140$^{-/-}$ mice (Supporting Figs. 6 and 7).

Discussion

Here, we report that miRNA-140$^{-/-}$ mice have increased NF-κB activity and are more prone to HCC development. In addition, we show that DDX20, an miRNP component, is frequently decreased in human HCC tissues. Because DDX20 deficiency preferentially causes impaired miRNA-140 function,[23] the functional impairment of miRNA-140 may result in phenotypes similar to those of miRNA-140$^{-/-}$ mice and may lead to hepatocarcinogenesis. In support of the hypothesis that DDX20 dysfunction is involved in hepatocarcinogenesis, DDX20 is located at 1p21.1-p13.2, a frequently deleted chromosomal region in human HCC,[27] and DDX20 was recently identified as a possible liver tumor suppressor in a functional screen in mice.[27] Although the possibility that intracellular signaling pathways other than miRNA-140 may also be involved in the biological consequences of DDX20 deficiency cannot be denied, we believe that functional impairment of miRNA-140 plays a major role in the phenotypes induced by DDX20 deficiency, based on the phenotypic similarities.

Changes in miRNA expression levels have been reported in various tumors.[7,12,42] However, in this study, we found that reduced expression of an miRNA machinery component might lead to carcinogenesis, at least in part, through functional impairment of miRNAs. Recent studies have shown that components of the RNA interference machinery are associated with the outcome of ovarian cancer patients,[43] and that single-nucleotide polymorphisms in miRNA machinery genes can be used as diagnostic risk markers.[44,45] Therefore, the impairment of miRNA function caused by deregulated miRNA machinery components may also be involved in carcinogenesis.

Our study identified Dnmt1 as a critical target of miRNA-140. The decreased MT expression due to the CpG promoter methylation induced by Dnmt1 resulted in enhanced NF-κB activity. This finding was consistent with the results obtained using MT gene knockout mice, in which enhanced NF-κB activation promoted hepatocarcinogenesis.[37] The decrease in MT expression that results from increased Dnmt1 expression caused by functional impairment of miRNA-140, together with increased NF-κB activation and hepatocarcinogenesis in MT knockout mice,[37] supports the concept that the DDX20/miRNA-140/Dnmt1/MT/NF-κB pathway may play a crucial role in hepatocarcinogenesis. However, we cannot fully exclude the possibility that other intracellular signaling pathways are also involved in the induction of hepatocarcinogenesis by miRNA-140 or DDX20 deficiency, because the precise role of NF-κB in hepatocarcinogenesis has not been clearly defined,[8] although constitutive activation of NF-κB signaling has been frequently detected in human HCCs.[46] The mechanisms by which DDX20 expression is initially decreased and the reason its locus is frequently deleted in HCC remain to be elucidated. However, because DDX20 expression is also regulated by methylation of its CpG promoter,[47] once this pathway is deregulated, decreased DDX20 expression could be maintained by a positive feedback mechanism, even without deletion of its locus.[27]

In conclusion, this study shows that miRNA-140 acts as a liver tumor suppressor. We show that DDX20, an miRNP component, is frequently decreased in human HCC, which may induce hepatocarcinogenesis via impairment of miRNA-140 function. These results suggest the importance of investigations of not only aberrant miRNA expression levels,[12,14,17,48] but also deregulation of miRNP

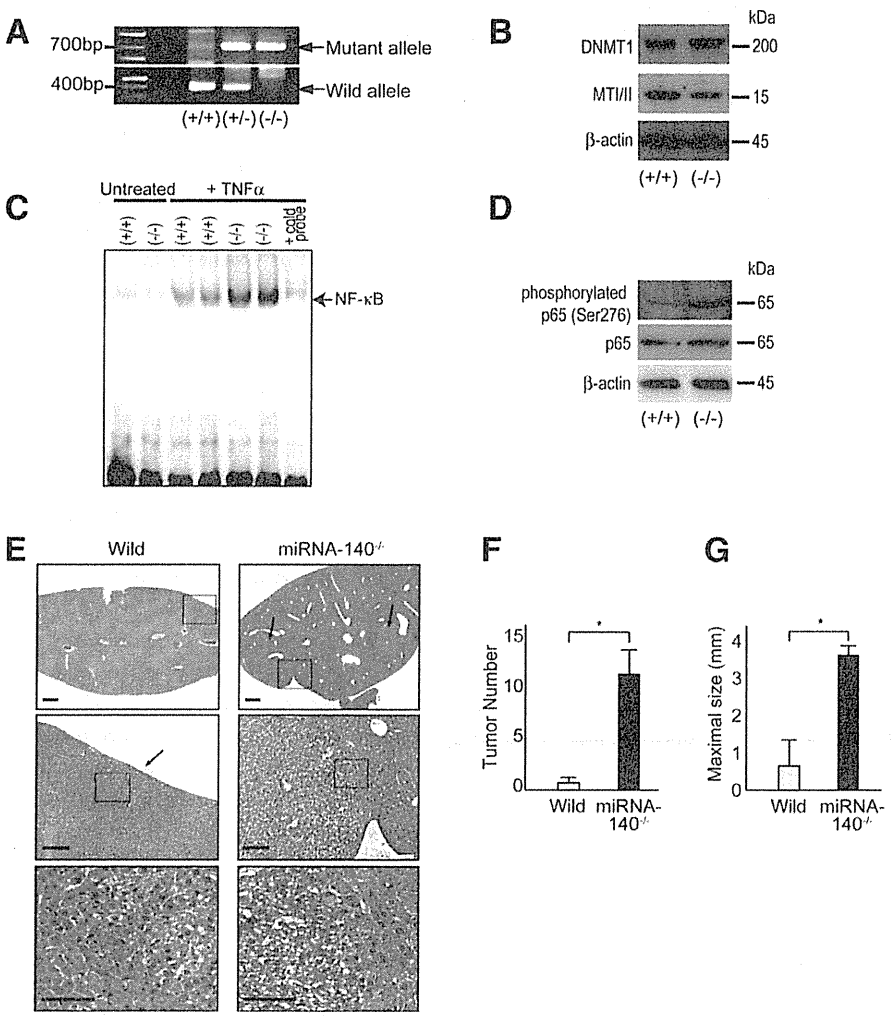

Fig. 4. miRNA-140$^{-/-}$ mice are prone to hepatocarcinogenesis. (A) Representative genotyping of mice with wild-type or mutant alleles. PCR genotyping was performed for miRNA-140 wild-type (419 bp; Wild) and knockout (734 bp; Mutant) alleles. (+/+), wild-type; (+/−), heterozygous; (−/−), knockout. (B) Increased Dnmt1 expression and decreased MTI/II expression in the liver tissues of miRNA-140$^{-/-}$ mice compared with wild-type mice. Western blotting was performed using antibodies against the indicated proteins. (+/+), wild-type; (−/−), miRNA-140$^{-/-}$. The image shown is representative of four independent experiments. (C) NF-κB–DNA binding was assessed via gel-shift assay using equal amounts of liver nuclear extracts from untreated and TNF-α–injected wild-type and miRNA-140$^{-/-}$ mice. (+/+), wild-type; (−/−), miRNA-140$^{-/-}$. Cold probe was added to TNF-α–injected knockout mouse nuclear extract to test assay specificity. A result representative of four independent experiments is shown. (D) Western blotting for phosphorylated p65 expression in the liver at 32 weeks after DEN treatment in miRNA-140$^{-/-}$ mice compared with wild-type mice. A result representative of four independent experiments is shown. (E) Representative histological images of mouse liver at 32 weeks after DEN treatment. Arrows indicate tumors. Higher-magnification images of the highlighted areas in the upper panels are shown in the lower panels. Scale bar, 500 μm. (F) The number (left panel) and size (right panel) of tumors (five random sections per mouse treated with DEN) are presented as the mean ± SD (wild-type mice, n = 8; miRNA-140$^{-/-}$ mice, n = 8). *$P < 0.05$.

components,[22] with subsequent impairment of miRNA function as molecular pathways and possible therapeutic targets for carcinogenesis and other diseases.

References

1. Parkin D, Bray F, Ferlay J, Pisani P. Global cancer statistics, 2002. CA Cancer J Clin 2005;55:74-108.
2. Block T, Mehta A, Fimmel C, Jordan R. Molecular viral oncology of hepatocellular carcinoma. Oncogene 2003;22:5093-5107.
3. Karin M. Nuclear factor-kappaB in cancer development and progression. Nature 2006;441:431-436.
4. Luedde T, Schwabe RF. NF-κB in the liver—linking injury, fibrosis and hepatocellular carcinoma. Nat Rev Gastroenterol Hepatol 2011;8:108-118.
5. Pikarsky E, Porat R, Stein I, Abramovitch R, Amit S, Kasem S, et al. NF-kappaB functions as a tumour promoter in inflammation-associated cancer. Nature 2004;431:461-466.
6. Liu P, Kimmoun E, Legrand A, Sauvanet A, Degott C, Lardeux B, et al. Activation of NF-kappa B, AP-1 and STAT transcription factors is a frequent and early event in human hepatocellular carcinomas. J Hepatol 2002;37:63-71.

7. Ji J, Shi J, Budhu A, Yu Z, Forgues M, Roessler S, et al. MicroRNA expression, survival, and response to interferon in liver cancer. N Engl J Med 2009;361:1437-1447.
8. Feng GS. Conflicting roles of molecules in hepatocarcinogenesis: paradigm or paradox. Cancer Cell 2012;21:150-154.
9. Bartel DP. MicroRNAs: target recognition and regulatory functions. Cell 2009;136:215-233.
10. Otsuka M, Jing Q, Georgel P, New L, Chen J, Mols J, et al. Hypersusceptibility to vesicular stomatitis virus infection in Dicer1-deficient mice is due to impaired miR24 and miR93 expression. Immunity 2007;27:123-134.
11. Otsuka M, Zheng M, Hayashi M, Lee JD, Yoshino O, Lin S, et al. Impaired microRNA processing causes corpus luteum insufficiency and infertility in mice. J Clin Invest 2008;118:1944-1954.
12. Kojima K, Takata A, Vadnais C, Otsuka M, Yoshikawa T, Akanuma M, et al. MicroRNA122 is a key regulator of α-fetoprotein expression and influences the aggressiveness of hepatocellular carcinoma. Nat Commun 2011;2:338.
13. Chang T-C, Yu D, Lee Y-S, Wentzel EA, Arking DE, West KM, et al. Widespread microRNA repression by Myc contributes to tumorigenesis. Nat Genet 2008;40:43-50.
14. Lu J, Getz G, Miska EA, Alvarez-Saavedra E, Lamb J, Peck D, et al. MicroRNA expression profiles classify human cancers. Nature 2005; 435:834-838.
15. Calin GA, Croce CM. MicroRNA signatures in human cancers. Nat Rev Cancer 2006;6:857-866.
16. Gaur A, Jewell DA, Liang Y, Ridzon D, Moore JH, Chen C, et al. Characterization of microRNA expression levels and their biological correlates in human cancer cell lines. Cancer Res 2007;67:2456-2468.
17. Kumar MS, Lu J, Mercer KL, Golub TR, Jacks T. Impaired microRNA processing enhances cellular transformation and tumorigenesis. Nat Genet 2007;39:673-677.
18. Lambertz I, Nittner D, Mestdagh P, Denecker G, Vandesompele J, Dyer MA, et al. Monoallelic but not biallelic loss of Dicer1 promotes tumorigenesis in vivo. Cell Death Differ 2010;17:633-641.
19. Otsuka M, Takata A, Yoshikawa T, Kojima K, Kishikawa T, Shibata C, et al. Receptor for activated protein kinase C: requirement for efficient microRNA function and reduced expression in hepatocellular carcinoma. PLoS One 2011;6:e24359.
20. Lujambio A, Esteller M. CpG island hypermethylation of tumor suppressor microRNAs in human cancer. Cell Cycle 2007;6:1455-1459.
21. Thomson J, Newman M, Parker J, Morin-Kensicki E, Wright T, Hammond S. Extensive post-transcriptional regulation of microRNAs and its implications for cancer. Genes Dev 2006;20:2202-2207.
22. Melo SA, Ropero S, Moutinho C, Aaltonen LA, Yamamoto H, Calin GA, et al. A TARBP2 mutation in human cancer impairs microRNA processing and DICER1 function. Nat Genet 2009;41:365-370.
23. Takata A, Otsuka M, Yoshikawa T, Kishikawa T, Kudo Y, Goto T, et al. A miRNA machinery component DDX20 controls NF-κB via microRNA-140 function. Biochem Biophys Res Commun 2012;13:564-569.
24. Miyaki S, Sato T, Inoue A, Otsuki S, Ito Y, Yokoyama S, et al. MicroRNA-140 plays dual roles in both cartilage development and homeostasis. Genes Dev 2010;24:1173-1185.
25. Garzon R, Heaphy CE, Havelange V, Fabbri M, Volinia S, Tsao T, et al. MicroRNA 29b functions in acute myeloid leukemia. Blood 2009;114:5331-5341.
26. Mourelatos Z, Dostie J, Paushkin S, Sharma A, Charroux B, Abel L, et al. miRNPs: a novel class of ribonucleoproteins containing numerous microRNAs. Genes Dev 2002;16:720-728.
27. Zender L, Xue W, Zuber J, Semighini C, Krasnitz A, Ma B, et al. An oncogenomics-based in vivo RNAi screen identifies tumor suppressors in liver cancer. Cell 2008;135:852-864.
28. Mouillet J, Yan X, Ou Q, Jin L, Muglia L, Crawford P, et al. DEAD-box protein-103 (DP103, Ddx20) is essential for early embryonic development and modulates ovarian morphology and function. Endocrinology 2008;149:2168-2175.
29. Voss M, Hille A, Barth S, Spurk A, Hennrich F, Holzer D, et al. Functional cooperation of Epstein-Barr virus nuclear antigen 2 and the survival motor neuron protein in transactivation of the viral LMP1 promoter. J Virol 2001;75:11781-11790.
30. Charroux B, Pellizzoni L, Perkinson R, Shevchenko A, Mann M, Dreyfuss G. Gemin3: a novel DEAD box protein that interacts with SMN, the spinal muscular atrophy gene product, and is a component of gems. J Cell Biol 1999;147:1181-1194.
31. Hutvágner G, Zamore P. A microRNA in a multiple-turnover RNAi enzyme complex. Science 2002;297:2056-2060.
32. Takata A, Otsuka M, Kojima K, Yoshikawa T, Kishikawa T, Yoshida H, et al. MicroRNA-22 and microRNA-140 suppress NF-κB activity by regulating the expression of NF-κB coactivators. Biochem Biophys Res Commun 2011;411:826-831.
33. Hu W, Johnson H, Shu H. Tumor necrosis factor-related apoptosis-inducing ligand receptors signal NF-kappaB and JNK activation and apoptosis through distinct pathways. J Biol Chem 1999;274: 30603-30610.
34. Cherian MG, Jayasurya A, Bay BH. Metallothioneins in human tumors and potential roles in carcinogenesis. Mutat Res 2003;533:201-209.
35. Huang GW, Yang LY. Metallothionein expression in hepatocellular carcinoma. World J Gastroenterol 2002;8:650-653.
36. Datta J, Majumder S, Kutay H, Motiwala T, Frankel W, Costa R, et al. Metallothionein expression is suppressed in primary human hepatocellular carcinomas and is mediated through inactivation of CCAAT/enhancer binding protein alpha by phosphatidylinositol 3-kinase signaling cascade. Cancer Res 2007;67:2736-2746.
37. Majumder S, Roy S, Kaffenberger T, Wang B, Costinean S, Frankel W, et al. Loss of metallothionein predisposes mice to diethylnitrosamine-induced hepatocarcinogenesis by activating NF-kappaB target genes. Cancer Res 2010;70:10265-10276.
38. Ghoshal K, Majumder S, Li Z, Dong X, Jacob ST. Suppression of metallothionein gene expression in a rat hepatoma because of promoter-specific DNA methylation. J Biol Chem 2000;275:539-547.
39. Harrington MA, Jones PA, Imagawa M, Karin M. Cytosine methylation does not affect binding of transcription factor Sp1. Proc Natl Acad Sci U S A 1988;85:2066-2070.
40. Li E, Beard C, Jaenisch R. Role for DNA methylation in genomic imprinting. Nature 1993;366:362-365.
41. Majumder S, Kutay H, Datta J, Summers D, Jacob ST, Ghoshal K. Epigenetic regulation of metallothionein-i gene expression: differential regulation of methylated and unmethylated promoters by DNA methyltransferases and methyl CpG binding proteins. J Cell Biochem 2006; 97:1300-1316.
42. Garzon R, Calin G, Croce C. MicroRNAs in cancer. Annu Rev Med 2009;60:167-179.
43. Merritt W, Lin Y, Han L, Kamat A, Spannuth W, Schmandt R, et al. Dicer, Drosha, and outcomes in patients with ovarian cancer. N Engl J Med 2008;359:2641-2650.
44. Horikawa Y, Wood CG, Yang H, Zhao H, Ye Y, Gu J, et al. Single nucleotide polymorphisms of microRNA machinery genes modify the risk of renal cell carcinoma. Clin Cancer Res 2008;14:7956-7962.
45. Yang H, Dinney CP, Ye Y, Zhu Y, Grossman HB, Wu X. Evaluation of genetic variants in microRNA-related genes and risk of bladder cancer. Cancer Res 2008;68:2530-2537.
46. Wu JM, Sheng H, Saxena R, Skill NJ, Bhat-Nakshatri P, Yu M, et al. NF-kappaB inhibition in human hepatocellular carcinoma and its potential as adjunct to sorafenib based therapy. Cancer Lett 2009;278: 145-155.
47. Gebhard C, Schwarzfischer L, Pham T, Andreesen R, Mackensen A, Rehli M. Rapid and sensitive detection of CpG-methylation using methyl-binding (MB)-PCR. Nucleic Acids Res 2006;34:e82.
48. Martello G, Rosato A, Ferrari F, Manfrin A, Cordenonsi M, Dupont S, et al. A microRNA targeting dicer for metastasis control. Cell 2010; 141:1195-1207.

Hepatitis C Virus NS3/4A Protease Inhibits Complement Activation by Cleaving Complement Component 4

Seiichi Mawatari[1], Hirofumi Uto[1*], Akio Ido[1], Kenji Nakashima[2], Tetsuro Suzuki[2], Shuji Kanmura[1], Kotaro Kumagai[1], Kohei Oda[1], Kazuaki Tabu[1], Tsutomu Tamai[1], Akihiro Moriuchi[1], Makoto Oketani[1], Yuko Shimada[3], Masayuki Sudoh[4], Ikuo Shoji[5], Hirohito Tsubouchi[6]

1 Digestive and Lifestyle Diseases, Department of Human and Environmental Sciences, Kagoshima University Graduate School of Medical and Dental Sciences, Kagoshima, Kagoshima, Japan, **2** Department of Infectious Diseases, Hamamatsu University School of Medicine, Hamamatsu, Shizuoka, Japan, **3** Miyazaki Prefectural Industrial Support Foundation, Miyazaki, Miyazaki, Japan, **4** Kamakura Research Division, Chugai Pharmaceutical, Co. Ltd., Kamakura, Kanagawa, Japan, **5** Division of Microbiology, Kobe University Graduate School of Medicine, Kobe, Japan, **6** Department of HGF Tissue Repair and Regenerative Medicine, Kagoshima University Graduate School of Medical and Dental Sciences, Kagoshima, Japan

Abstract

Background: It has been hypothesized that persistent hepatitis C virus (HCV) infection is mediated in part by viral proteins that abrogate the host immune response, including the complement system, but the precise mechanisms are not well understood. We investigated whether HCV proteins are involved in the fragmentation of complement component 4 (C4), composed of subunits C4α, C4β, and C4γ, and the role of HCV proteins in complement activation.

Methods: Human C4 was incubated with HCV nonstructural (NS) 3/4A protease, core, or NS5. Samples were separated by sodium dodecyl sulfate-polyacrylamide gel electrophoresis and then subjected to peptide sequencing. The activity of the classical complement pathway was examined using an erythrocyte hemolysis assay. The cleavage pattern of C4 in NS3/4A-expressing and HCV-infected cells, respectively, was also examined.

Results: HCV NS3/4A protease cleaved C4γ in a concentration-dependent manner, but viral core and NS5 did not. A specific inhibitor of NS3/4A protease reduced C4γ cleavage. NS3/4A protease–mediated cleavage of C4 inhibited classical pathway activation, which was abrogated by a NS3/4A protease inhibitor. In addition, co-transfection of cells with C4 and wild-type NS3/4A, but not a catalytic-site mutant of NS3/4A, produced cleaved C4γ fragments. Such C4 processing, with a concomitant reduction in levels of full-length C4γ, was also observed in HCV-infected cells expressing C4.

Conclusions: C4 is a novel cellular substrate of the HCV NS3/4A protease. Understanding disturbances in the complement system mediated by NS3/4A protease may provide new insights into the mechanisms underlying persistent HCV infection.

Citation: Mawatari S, Uto H, Ido A, Nakashima K, Suzuki T, et al. (2013) Hepatitis C Virus NS3/4A Protease Inhibits Complement Activation by Cleaving Complement Component 4. PLoS ONE 8(12): e82094. doi:10.1371/journal.pone.0082094

Editor: Ferruccio Bonino, University of Pisa, Italy

Received September 20, 2013; **Accepted** October 11, 2013; **Published** December 12, 2013

Funding: This study was supported by a Grant-in-Aid for Research on Hepatitis and BSE from the Ministry of Health, Labour and Welfare of Japan; a grant for Scientific Research from the Ministry of Education, Culture, Sports, Science and Technology of Japan; and a grant from the Miyazaki Prefecture Collaboration of Regional Entities for the Advancement of Technological Excellence. The funders had no role in study design, data collection and analysis, decision to publish, or preparation of the manuscript.

Competing interests: The authors disclose the following: M. Sudoh is employee of Chugai Pharmaceutical Co., Ltd. H. Tsubouchi holds endowed faculty position in research for HGF tissue repair and regenerative medicine, and has received funds from Eisai Co., Ltd. The remaining authors disclose no conflicts. This does not alter the authors' adherence to all the PLOS ONE policies on sharing data and materials.

* E-mail: hirouto@m2.kufm.kagoshima-u.ac.jp

Introduction

Hepatitis C virus (HCV) is a single-stranded positive-strand RNA virus of the Flaviviridae family. The viral genome encodes four structural proteins and six non-structural (NS) proteins [1]. NS3/4A, a complex consisting of NS3 with serine protease activity and cofactor NS4A, plays an essential role in processing of HCV proteins. NS3/4A is a target of direct-acting antiviral agents (DAA) [2,3], and use of an NS3/4A protease inhibitor as a DAA markedly increases the therapeutic effect of other anti-HCV agents. Thus, NS3/4A protease may play an important role in interfering with the antiviral response.

HCV has been hypothesized to block the host immune response against persistent infection [4]. Furthermore, the time required for HCV-infected patients to develop hepatic cirrhosis varies among individuals; in particular, the progression of

hepatic fibrosis seems to be slower in HCV carriers with persistent normal alanine aminotransferase (ALT) levels than in chronic hepatitis patients with elevated ALT levels [5]. These differences in clinical features might be caused by variations in the host immune response, but the underling mechanism is unclear.

In the course of proteomic analyses aimed at identifying proteins potentially involved in the pathophysiology of hepatic diseases, we found that a specific peptide fragment of complement component 4 (C4) was significantly more abundant in HCV carriers with persistent normal ALT than in patients with chronic hepatitis [6], as well as more abundant in HCV carriers, regardless of ALT levels, compared to healthy controls. Assuming that C4 expression levels are similar among these groups, this C4 fragment may be generated by post-translational processing in HCV-infected individuals.

The complement system is part of the innate immune system, which can be activated through three pathways: the classical pathway, the mannose-binding lectin pathway, and the alternative pathway. C4, which is involved in the classical- and mannose-binding lectin pathways, can be cleaved by certain cellular protease(s), leading to a cascade of C4 activation [7]. In this study, we provide the first evidence that HCV NS3/4A cleaves C4, and that this cleavage attenuates activation of the classical pathway of complement system.

Materials and Methods

Materials

HCV NS3/4A protease (217 amino acid [aa] fusion protein with NS4A co-factor fused to the N-terminus of NS3 protease domain) with His-tag, HCV core (aa 1–102) with GST-tag, and HCV NS5 (aa 2061–2302) with GST-tag were purchased from AnaSpec (Fremont, CA) or ProSpec (Rehovot, Israel). Isolated human-derived complement components (C1, C2) were obtained from Hycult Biotech (Uden, Netherlands), and C4 and C4-deficient guinea pig serum (C4d-GPS) were purchased from Sigma-Aldrich (St. Louis, MO). VX950, a HCV NS3/4A serine protease inhibitor, was obtained from Selleck Chemicals (Houston, TX). Veronal buffer, sheep erythrocytes, and hemolysin were purchased from Wako (Osaka, Japan), Nippon Biotest Laboratories Inc. (Tokyo, Japan), and Denka Seiken Co. (Tokyo, Japan), respectively.

NS3/4A protease cleavage assay

HCV NS3/4A protease, core, or NS5 (3 μl) and 9 μl of Assay buffer (SensoLyte® 490 HCV Protease Assay Kit, AnaSpec) containing 30 mM dithiothreitol (DTT) were added to C4 (3 μl), and the mixture was incubated at 30°C for 30 min. The solution was separated by sodium dodecyl sulfate polyacrylamide gel electrophoresis (SDS-PAGE), and resolved proteins were stained with Coomassie brilliant blue (CBB). In a separate experiment, VX950 was pre-incubated with NS3/4A protease at 30°C for 30 min, and then incubated with C4 at 30°C for 30 min. Proteins detected by CBB staining were subjected to N-terminal peptide sequence analysis at Nippi Inc. (Tokyo, Japan).

Hemolytic analysis

The method used for hemolytic analysis has been described previously [8,9]. Briefly, intermediates of complement components were sequentially added to sheep erythrocytes sensitized by hemolysin (Ab-sensitized sheep erythrocytes, EA). Dilute erythrocytes and complement components were prepared in Veronal buffer containing 2% gelatin (GVB). To prepare EA, hemolysin was added to 10 ml of erythrocytes (5×10^8 cells/ml) and incubated at 37°C for 30 min. C1 (10 μg) was added to 5 ml of EA, incubated at 30°C for 15 min, and washed twice with GVB (EAC1). NS3/4A protease was prepared in a solution containing 20 mM Tris-HCl (pH 8.0), 20% glycerol, 100 mM KCl, 1 mM DTT, and 0.2 mM EDTA, adjusted to pH 7.5. The reaction solution was adjusted to 2 mM DTT to ensure a uniform effect on C4 activity. C4 was incubated with the NS3/4A protease, and then mixed with 100 μl of EAC1 and incubated at 30°C for 15 min (EAC1-C4). After washing twice with GVB, 1 μl of C2 (0.1 mg/ml) was added and the mixture was incubated at room temperature for 4 min (EAC1-C4-C2). After washing twice again with GVB, 150 μl of 80-fold diluted C4d-GPS was added to 30 μl of EAC1-C4-C2, and the mixture was incubated at 37°C for 30 min. The optical absorbance of the centrifuged supernatant was determined at 415 nm, and the level of hemolysis was calculated using the following formula: Hemolysis (%) = (sample OD_{415} – no C4 OD_{415})/(total hemolysis in distilled water OD_{415} – no C4 OD_{415}) ×100. "No C4" refers to a control sample containing EAC1 not incubated with C4. In a separate experiment, VX950 was first pre-incubated with NS3/4A protease at 30°C for 30 min, and then incubated with C4 at 30°C for 30 min.

Cell culture and transfection

Human hepatoma-derived Huh7.5.1 cells (a kind gift from Dr. F. V. Chisari, The Scripps Research Institute, La Jolla, CA) and human embryonic kidney (HEK) 293T cells were cultured at 37°C under 5% CO_2 in DMEM containing 10% FBS, 100 units/ml penicillin, and 100 g/ml streptomycin. DNA transfections of Huh7.5.1 cells and 293T cells were performed using Lipofectamine LTX/PLUS Reagent (Invitrogen, Carlsbad, CA) and polyethylenimine (Alfa Aesar, Heysham, Lancashire, UK), respectively. The transfection complex was formed at a DNA:reagent ratio of 1:1 (w/w) in OptiMEM (Invitrogen) with incubation for 15 min at room temperature before it was added to the culture.

Preparation of virus stock

The pJ6/JFH1 plasmid was generated by replacing the structural region of the JFH-1 strain with that of the J6CF strain, as described [10]. Cell culture–derived infectious HCV particles (HCVcc) were produced by introducing *in vitro* transcribed RNA from pJ6/JFH1 into Huh-7.5.1 cells by electroporation. The culture supernatant was concentrated using a 100-kDa MWCO Amicon Ultra Centrifugal Filter (Millipore, Bedford, MA). Virus infectivity was measured by indirect immunofluorescence analysis. Virus stocks (1×10^7 focus-forming units/ml) were divided into small aliquots and stored at −80 °C until use.

Plasmids

The C4 expression plasmid pFN21-C4A was purchased from Kazusa DNA Research Institute (Kisarazu, Japan). To create pFN21-C4A delH-Tag, the N-terminal Halo-Tag of pFN21-C4A was removed by digestion with *Hind*III and *Pvu*I, followed by blunt-ending with KOD FX neo (Toyobo, Osaka, Japan). pCAG-HA-NS3/4A, which expresses full-length NS3 and NS4 (derived from HCV genotype 1b, Con-1 strain) with an HA tag at the N-terminus of NS3 was generated as described [11]. Point mutation of serine to alanine at position 139 (S139A) in pCAG-HA-NS3/4A was achieved by site-directed mutagenesis using two primers: 5′-TAC TTG AAG GGC TCT GCG GGC GGT CCA CTG C-3′ and 5′-GCA GTG GAC CGC CCG CAG AGC CCT TCA AGT A-3′. The point mutation was confirmed by DNA sequencing.

Immunoprecipitation and immunoblotting

Goat anti-human complement C4 antibody (MP Biomedicals, Santa Ana, CA) was bound to protein G–agarose beads (Thermo Scientific, Rockford, IL) in binding buffer (0.5% Nonidet P-40, 25 mM Tris [pH 7.5], 150 mM NaCl, 1 mM EDTA and protease inhibitor cocktail [Roche, Basel, Switzerland]) for 1 h at room temperature. Culture supernatants were incubated with the beads for 1 h at room temperature, and the immunoprecipitated proteins were eluted by heat treatment for 5 min at 100°C with 2× sample buffer. Culture supernatants were directly mixed with 3× sample buffer at a ratio of 1 volume supernatant to 2 volumes sample buffer (1:2 [v/v]). Cells were solubilized in lysis buffer (1% Triton X-100, 25 mM Tris, pH 7.5, 150 mM NaCl, 1 mM EDTA and protease inhibitor cocktail) on ice. Cell debris was removed by centrifugation, and the resultant supernatants were diluted 1:2 (v/v) with 3× sample buffer. Precipitated proteins, culture supernatants, and cell lysates were separated by SDS-PAGE and transferred to polyvinylidene difluoride (PVDF) membranes (Immobilon-P, Millipore). After blocking in 4% BlockAce (DS Pharma Biomedical, Osaka, Japan), the blots were incubated with the indicated primary antibodies, followed by the secondary antibody in TBST (25 mM Tris [pH 7.5], 150 mM NaCl, and 0.1% Tween 20). The primary antibodies used were anti-C4γ (clone H-291, Santa Cruz Biotechnology, Dallas, TX), anti-human complement C4, anti-HA (Sigma, St. Louis, MO), anti-HCV core (clone 2H9) and anti-GAPDH (clone 6C5, Santa Cruz Biotechnology). Donkey polyclonal Secondary Antibody to Goat IgG-H&L (HRP) (Abcam, Cambridge, UK), HRP-linked anti-mouse IgG, and HRP-linked anti–rabbit IgG (Cell Signaling Technology, Danvers, MA) were used as secondary antibodies. Finally, proteins were visualized using an enhanced chemiluminescence (ECL) reagent (ECL Select Western Blotting Detection Reagent, GE Healthcare, Little Chalfont, UK).

Statistical analysis

The concentration of proteins detected by Western blots was determined by densitometric analysis using the ImageJ software [12]. Statistical analysis was performed with the SPSS software (SPSS Inc., Chicago, IL) using the Tukey test, with $P < 0.05$ considered to indicate a significant difference.

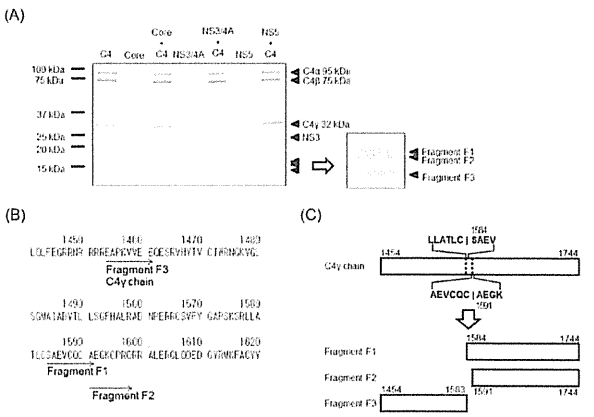

Figure 1. C4 is cleaved by HCV NS3/4A protease at Cys-1583/Ser-1584 or Cys-1590/Ala-1591. (A) HCV NS3/4A protease, core, or NS5 was added to C4, and the products were separated by SDS-PAGE and subjected to CBB staining. Two approximately 17-kDa proteins (Fragment F1 and F2) and a 15-kDa protein (Fragment F3) were detected after incubation of C4 with HCV NS3/4A protease, but not after incubation with core or NS5. (B) Amino acid sequence of aa 1451-1620 region of C4. Protein fragments were analyzed by N-terminal peptide sequencing. The sequences of the N-termini of the 17-kDa proteins (Fragment F1 and F2) were SAEVCQCA and AEGKCPRQ, which are located at aa 1584–1591 and 1591–1598 in C4, respectively. The sequence of the N-terminus of the 15-kDa protein (Fragment F3) was EAPKVVEE, which is located at aa 1454–1461 in C4. (C) Schematic representation of C4γ chain, and Fragment F1, F2 and F3.

doi: 10.1371/journal.pone.0082094.g001

Results

HCV NS3/4A protease cleaves C4 in vitro

To test cleavage of C4 mediated by HCV proteins, C4 (containing subunits C4α, C4β, and C4γ) was mixed with NS3/4A protease, core, or NS5, followed by incubation at 30°C for 30 min. As shown in Figure 1A, doublet bands at 17 kDa (fragments F1 and F2 in the enlarged view) and one band at 15 kDa (fragment F3) were detected in the presence of NS3/4A protease and C4. These bands were not detected after incubation of C4 with core or NS5, or when either core or NS5 were incubated alone.

N-terminal sequence analyses revealed that the bands at approximately 100, 75, and 32 kDa (Figure 1A) represented C4α (N-terminus sequence identified: NVNFQKAI), C4β (KPRLLLFS), and C4γ (EAPKVVEE), respectively. As shown in Figure 1B, the N-terminal sequences of the doublet proteins at 17 kDa were identical to sequences found in C4γ: SAEVCQCA (aa 1584–1591 of C4) and AEGKCPRQ (aa 1591–1598). In addition, the N-terminal sequence of the 15-kDa fragment was EAPKVVEE (aa 1454–1461), indicating that the 15-kDa fragment is the N-terminal region of the C4γ. These results demonstrate that HCV NS3/4A protease cleaves C4 between

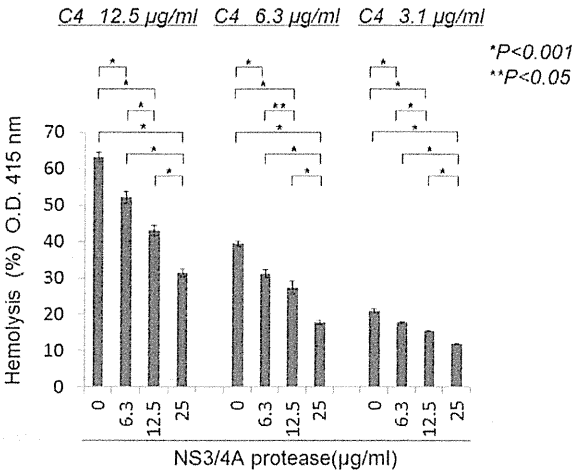

Figure 2. HCV NS3/4A protease inhibits the classical pathway, as assessed by hemolysis. C4 was incubated in the presence or absence of HCV NS3/4A protease, and then C1-sensitized EA (EAC1) was added (EAC1-C4). After washing, C2 was added to form EAC1-C4-C2, and the complex was resuspended in C4d-GPS. The absorbance of the centrifuged supernatant was determined at 415 nm. The grade of hemolysis decreased in the presence of NS3/4A protease in a dose-dependent manner. All measurements were performed in triplicate, and data are expressed as means ± SD.

doi: 10.1371/journal.pone.0082094.g002

either Cys-1583 and Ser-1584 or Cys-1590 and Ala-1591, consistent with the consensus sequence of HCV NS3 proteinase cleavage sites [3,13]. Possible locations for the 15- and 17-kDa fragments of C4γ are shown in Figure 1B and 1C.

HCV NS3/4A protease decreases the activity of the classical pathway of the complement system in a concentration-dependent manner

To examine the functional significance of C4 cleavage by NS3/4A protease, complement components were serially added to EA to reproduce the classical pathway of the complement system. C4, untreated or treated with various concentrations of NS3/4A, was added at various concentrations to the EA-C1 mixture, followed by addition of C2 and C4d-GPS, which were used as sources of C3 and C5-C9. Erythrocyte hemolysis, which is caused by the complement-mediated fusion of erythrocytes, was quantified (Figure 2). NS3/4A treatment significantly decreased hemolysis levels in a concentration-dependent manner. This result, together with those in Figure 1, suggests that the C4 cleavage mediated by NS3/4A protease may contribute to inhibition of complement activation via the classical pathway.

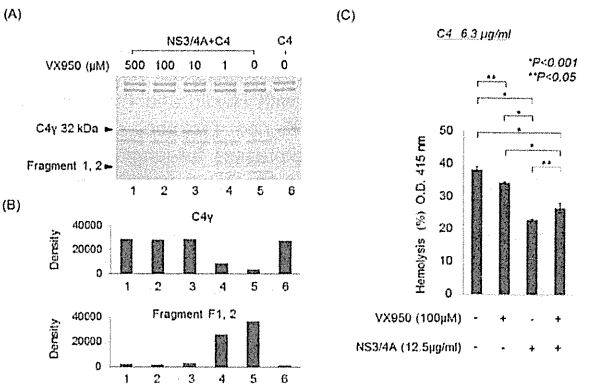

Figure 3. VX950, a HCV NS3/4A protease inhibitor, abrogates cleavage of C4 induced by HCV NS3/4A protease. (A) VX950 was added to HCV NS3/4A protease at the indicated concentrations, and then C4 was added. Proteins were separated by SDS-PAGE for CBB staining. The three C4-derived fragments of 17 kDa and 15 kDa produced by NS3/4A protease action could not be detected after pretreatment with VX950, and this change was accompanied by an increased concentration of the 32-kDa C4γ chain. (B) The C4γ, 17-kDa, and 15-kDa bands were quantified by densitometric analysis using the Image J software. (C) C4 was incubated in the presence or absence of HCV NS3/4A or VX950, and then C1-sensitized EA (EAC1) was added (EAC1–C4). C2 and C4d-GPS were then added, and the absorbance of the supernatant was determined at 415 nm. Hemolysis was inhibited by NS3/4A protease and this inhibition was blocked by VX950. All measurements were made in triplicate, and data are expressed as means ± SD.

doi: 10.1371/journal.pone.0082094.g003

HCV protease inhibitor reduces inactivation of complement by blocking C4 cleavage by NS3/4A protease

We tested the effect of VX950, a specific inhibitor of NS3/4A protease, on C4 cleavage by NS3/4A protease and inhibition of complement activation. As shown in Figure 3A and 3B, under a condition in which more than 80% of 32-kDa C4γ was processed into 17- and 15-kDa fragments in the presence of NS3/4A protease (lanes 5), pretreatment of the protease with 1 μM VX950 moderately inhibited the cleavage of C4γ (lanes 4). The NS3/4A-mediated processing of C4γ into 17- and 15-kDa fragments was almost completely blocked by VX950 at ≥10 μM (lanes 1–3). In the erythrocyte hemolysis assay, the reduction in hemolysis level mediated by NS3/4A significantly recovered in the presence of VX950 (Figure 3C). These results confirmed cleavage of C4γ by NS3/4A and the involvement of the protease in the classical complement pathway.

Cleavage of C4γ in NS3/4A-expressing cells and HCV-infected cells

To determine whether HCV NS3/4A protease cleaves C4 in cells, we analyzed 32-kDa C4γ and its processed fragments in

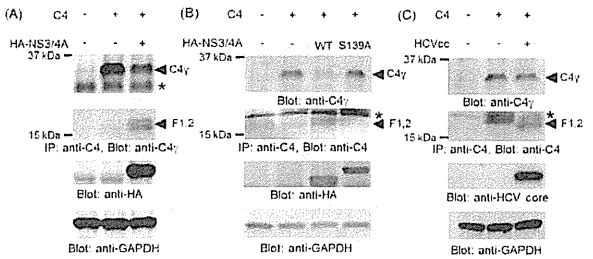

Figure 4. C4 is cleaved by HCV NS3/4 protease in cell cultures. (A) 293T cells were transfected with the indicated plasmids. Anti-C4 immunoprecipitates (IP) of supernatants were separated by SDS-PAGE and analyzed by immunoblotting with anti-C4γ antibody. Detergent-soluble cell lysates were separated by SDS-PAGE and analyzed by immunoblotting with anti-HA and anti-GAPDH antibodies. (B) 293T cells were transfected with the indicated plasmids. Culture supernatants were analyzed by immunoblotting with anti-C4γ antibody. Anti-C4 immunoprecipitates (IP) of supernatants were analyzed by immunoblotting with anti-C4 antibody. Detergent-soluble cell lysates were analyzed by immunoblotting with anti-HA and anti-GAPDH antibodies. (C) Huh7.5.1 cells were mock-infected or infected with HCVcc at a multiplicity of infection of 2 for 6 h, followed by mock-transfection or transfection with C4 expression plasmid. Culture supernatants and cell lysates were analyzed as described in (A) and (B). The anti-C4γ antibody was not appropriate for immunoblotting of IP samples derived from Huh7.5.1 cultures because of unavoidable nonspecific cross-reaction. * indicates non-specific reactions in (A) – (C).

doi: 10.1371/journal.pone.0082094.g004

culture medium from 293T cells cotransfected with expression plasmids encoding C4 (pFN21-C4A delH-Tag) and NS3/4A protease (pCAG-HA-NS3/4A). Co-expression of C4 and NS3/4A derived from HCV genotype 1b led to production of the 17-kDa C4γ fragment and reduction in the level of 32-kDa C4γ (Figure 4A). In contrast, the 17-kDa fragment was not detected, and the 32-kDa C4γ level was not changed, when a mutant NS3 with an amino-acid substitution at the catalytic-site (S139A)/4A was co-expressed with C4 (Figure 4B). Next, we investigated C4 cleavage in HCV-infected cultures. In the culture medium of Huh7.5.1 cells infected with HCVcc of strain J6/JFH-1 (genotype 2a) expressing of C4 from pFN21-C4A delH-Tag, the 17-kDa fragment was produced, and the level of 32-kDa C4γ was reduced accordingly (Figure 4C). These data demonstrate that C4γ can be cleaved by HCV NS3/4A, either expressed from a plasmid or in HCV-infected cells, and that proteases of both genotypes 1b and 2a are functional in this cleavage.

Discussion

The results of this study show that C4γ is cleaved by HCV NS3/4A protease *in vitro* and in cell culture. Cleavage of C4 by HCV NS3/4A protease leads to inhibition of activity of the classical complement pathway. C4 cleavage and abrogation of complement activation are blocked by an inhibitor of NS3/4A protease.

HCV NS3/4A protease plays an important role in the replication of non-structural regions [2,3], and might also directly act on the IFN signaling system to inhibit the host immune response and prevent viral clearance, thereby contributing to persistent HCV infection. However, a direct relationship between HCV infection and complement components has not been previously established. Levels of functional C3 or C4 assessed by hemolysis assay are reduced after infection by flaviviruses such as Dengue virus and West Nile virus (WNV) [9,14]. In mice infected with γ-herpesvirus or WNV, genetic deletion of complement C3 or C4 not only enhances mortality but also increases persistent replication of γ-herpesvirus or WNW RNA levels [14,15]. Furthermore, Moulton et al. reported that mousepox virus dissemination was more severe, and viral loads in tissues were higher, in C3-deficient mice; leading to higher mortality than in wild-type mice; those authors concluded that the complement system is critical for slowing viral spread and decreasing tissue titer and damage [16]. Thus, it is likely that the complement system is widely associated with development of viral infection. Further investigation of the role of complement activation mediated by HCV proteins such as HCV NS3/4A protease may provide new insights into development of persistent HCV infection.

Our results indicated that the C4 cleavage site of HCV NS3/4A protease is between either Cys-1583 and Ser-1584 or Cys-1590 and Ala-1591 of C4, both of which are located in the C4γ chain (Figure 1). HCV NS3/4A protease has previously been suggested to cleave at Cys/Thr and Ala/Ser sites [3,13], which is broadly consistent with our results. C4 was also cleaved by HCV NS3/4A protease in HCV-infected cells (Figure 4C), in which unprocessed 32-kDa C4γ and cleaved 17-kDa fragment in the culture medium were observed. In cultures of human hepatoma HepG2 cells, the major fraction of C4α, C4β, and C4γ were present in the culture medium rather than in cells [17,18]. In good agreement with that finding, we detected little C4 in Huh-7–derived cells (data not shown). We speculate that immediately after synthesis, at least a fraction of C4γ can be quickly cleaved by NS3/4A in virally replicating cells, followed by secretion into the culture medium. However, we cannot rule out the possibility that HCV NS3/4A protease is present extracellularly and is functional under some particular conditions, because addition of recombinant antigens derived from the NS3 region to NS4 improves the sensitivity of the anti-HCV test in serum and shortens the window period for seroconversion in patients infected with HCV [19].

Complement components are involved in innate immunity and are responsible for one of the major immunological mechanisms mediated by antibodies [7]. In viral and bacterial infection, these components cause lysis of the outer membrane of virus particles [20] and infected cells [21] by the membrane attack complex C5–C9, ultimately resulting in elimination of the pathogen. Some viruses, such as cytomegalovirus, induce expression of cellular complement inhibitors, for example, decay-accelerating factor and monocyte chemoattractant protein, leading to increased levels of these proteins on the

surfaces of infected cells. Human immunodeficiency virus may incorporate the complement inhibitors into the viral envelope [22,23]. NS1 protein secreted from flaviviruses, such as dengue virus, West Nile virus, and yellow fever virus, not only attenuates activation of the classical and lectin pathways by directly interacting with C4, but also inactivates C4b by interacting with C4-binding protein [9,24]. Thus, NS1 of flaviviruses is considered to play a role in protecting the virus from complement-dependent neutralization. To our knowledge, however, our study provides the first evidence that the viral protease plays a role in protecting the virus from the complement defense system via proteolytic processing of the complement component.

In particular, C4 is involved in the classical and mannose-binding lectin pathways of the complement system, and it is responsible for the major activity of complement components. Upon antibody binding to an antigen, C4 is cleaved into C4a and C4b by the C1q-C1r-C1s complex, and C4b then binds to C2a (C4b2a) on the cell membrane to cleave C3 into C3a and C3b. Subsequently, C3b binds to C4b2a to cleave C5, and finally C5b and C6-C9 form the membrane attack complex to cause lysis of the cell membrane [7]. The erythrocyte hemolysis assay used in this study reproduces this cascade and revealed that HCV NS3/4A protease cleaves C4 and decreases the activity of the classical pathway. The specific assay was constructed to evaluate the function of C4 in the classical pathway by allowing HCV NS3/4A protease to act on C4 alone, without influence from other complement components. Therefore, further work is needed to determine whether HCV NS3/4A protease affects other components.

Several studies have demonstrated that HCV proteins influence complement systems and may be involved in evading antiviral immune responses of the host, as follows. Amet et al. reported that CD59, which may inhibit formation of the membrane attack complex, is incorporated into cultured cells and plasma primary HCV virions and inhibited activation of complement components, whereas administration of a CD59 inhibitor increases the sensitivity of component activation against endogenous HCV viral particles [25]. Banerjee et al. found that the HCV core protein reduces the expression of upstream stimulatory factor (USF)-1, a transcription factor important for basal C4 expression, and that expression of interferon regulatory factor (IRF)-1, which is important for IFN-γ–induced C4 expression, is inhibited by hepatocytes expressing HCV NS5A [26]. Mazumdar et al. showed that NS5A strongly downregulates C3 promoter activity in the presence of IL-1β, acting as an inducer [27]. HCV core inhibits T-cell proliferative responses *in vitro*, and this effect can be reversed by addition of anti–C1q receptor antibody to a T-cell proliferation assay [28]. Here, we identified C4γ as a novel cellular substrate of the HCV NS3/4A protease.

The results of this study suggest that C4γ cleavage by NS3/4A decreased the activity of the classical complement pathway, and might thereby attenuate activation of the complement system. An understanding of the viral protease–mediated inhibition of the complement system should provide new insights into the roles played by immune evasion in persistent HCV infection.

Acknowledgements

We wish to thank the Joint Research Laboratory, Kagoshima University Graduate School of Medical and Dental Sciences, for the use of their facilities.

Author Contributions

Conceived and designed the experiments: SM HU YS MS HT. Performed the experiments: SM KN TS SK KK KO KT TT AM MO. Analyzed the data: SM HU AI KN TS YS. Contributed reagents/materials/analysis tools: HU IS HT. Wrote the manuscript: SM HU TS HT.

References

1. Rehermann B (2009) Hepatitis C virus versus innate and adaptive immune responses: a tale of coevolution and coexistence. J Clin Invest 119: 1745-1754. doi:10.1172/JCI39133. PubMed: 19587449.
2. Moradpour D, Penin F, Rice CM (2007) Replication of hepatitis C virus. Nat Rev Microbiol 5: 453-463. doi:10.1038/nrmicro1645. PubMed: 17487147.
3. Morikawa K, Lange CM, Gouttenoire J, Meylan E, Brass V et al. (2011) Nonstructural protein 3-4A: the Swiss army knife of hepatitis C virus. J Viral Hepat 18: 305-315. doi:10.1111/j.1365-2893.2011.01451.x. PubMed: 21470343.
4. Barnaba V (2010) Hepatitis C virus infection: a "liaison a trois" amongst the virus, the host, and chronic low-level inflammation for human survival. J Hepatol 53: 752-761. doi:10.1016/j.jhep.2010.06.003. PubMed: 20673595.
5. Persico M, Perrotta S, Persico E, Terracciano L, Folgori A et al. (2006) Hepatitis C virus carriers with persistently normal ALT levels: biological peculiarities and update of the natural history of liver disease at 10 years. J Viral Hepat 13: 290-296. doi:10.1111/j.1365-2893.2005.00667.x. PubMed: 16637858.
6. Imakiire K, Uto H, Sato Y, Sasaki F, Mawatari S et al. (2012) Difference in serum complement component C4a levels between hepatitis C virus carriers with persistently normal alanine aminotransferase levels or chronic hepatitis C. Mol Med Rep 6: 259-264. PubMed: 22614103.
7. Walport MJ (2001) Complement. First of two parts. N Engl J Med 344: 1058-1066. doi:10.1056/NEJM200104053441406. PubMed: 11287977.
8. Krych-Goldberg M, Hauhart RE, Subramanian VB, Yurcisin BM 2nd, Crimmins DL et al. (1999) Decay accelerating activity of complement receptor type 1 (CD35). Two active sites are required for dissociating C5 convertases. J Biol Chem 274: 31160-31168. doi:10.1074/jbc.274.44.31160. PubMed: 10531307.
9. Avirutnan P, Fuchs A, Hauhart RE, Somnuke P, Youn S et al. (2010) Antagonism of the complement component C4 by flavivirus nonstructural protein NS1. J Exp Med 207: 793-806. doi:10.1084/jem.20092545. PubMed: 20308361.
10. Murayama A, Weng L, Date T, Akazawa D, Tian X et al. (2010) RNA polymerase activity and specific RNA structure are required for efficient HCV replication in cultured cells. PLoS Pathog 6:e1000885. PubMed: 20442786.
11. Matsui C, Shoji I, Kaneda S, Sianipar IR, Deng L et al. (2012) Hepatitis C virus infection suppresses GLUT2 gene expression via downregulation of hepatocyte nuclear factor 1α. J Virol 86: 12903-12911. doi:10.1128/JVI.01418-12. PubMed: 22993150.
12. Schneider CA, Rasband WS, Eliceiri KW (2012) NIH Image to ImageJ: 25 years of image analysis. Nat Methods 9: 671-675. doi:10.1038/nmeth.2089. PubMed: 22930834.
13. Bartenschlager R, Ahlborn-Laake L, Yasargil K, Mous J, Jacobsen H (1995) Substrate determinants for cleavage in cis and in trans by the hepatitis C virus NS3 proteinase. J Virol 69: 198-205. PubMed: 7983710.
14. Mehlhop E, Diamond MS (2006) Protective immune responses against West Nile virus are primed by distinct complement activation pathways.

J Exp Med 203: 1371-1381. doi:10.1084/jem.20052388. PubMed: 16651386.
15. Kapadia SB, Levine B, Speck SH, Virgin HW 4th (2002) Critical role of complement and viral evasion of complement in acute, persistent, and latent gamma-herpesvirus infection. Immunity 17: 143-155. doi: 10.1016/S1074-7613(02)00369-2. PubMed: 12196286.
16. Moulton EA, Atkinson JP, Buller RM (2008) Surviving mousepox infection requires the complement system. PLoS Pathog 4:e1000249. PubMed: 19112490.
17. Chan AC, Atkinson JP (1983) Identification and structural characterization of two incompletely processed forms of the fourth component of human complement. J Clin Invest 72: 1639-1649. doi: 10.1172/JCI111123. PubMed: 6313766.
18. Andoh A, Fujiyama Y, Bamba T, Hosoda S (1993) Differential cytokine regulation of complement C3, C4, and factor B synthesis in human intestinal epithelial cell line, Caco-2. J Immunol 151: 4239-4247. PubMed: 8409399.
19. Mattsson L, Gutierrez RA, Dawson GJ, Lesniewski RR, Mushahwar LK et al. (1991) Antibodies to recombinant and synthetic peptides derived from the hepatitis C virus genome in long-term-studied patients with posttransfusion hepatitis C. Scand J Gastroenterol 26: 1257-1262. doi: 10.3109/00365529108998622. PubMed: 1722348.
20. Sullivan BL, Knopoff EJ, Saifuddin M, Takefman DM, Saarloos MN et al. (1996) Susceptibility of HIV-1 plasma virus to complement-mediated lysis. Evidence for a role in clearance of virus in vivo. J Immunol 157: 1791-1798. PubMed: 8759769.
21. Terajima M, Cruz J, Co MD, Lee JH, Kaur K et al. (2011) Complement-dependent lysis of influenza a virus-infected cells by broadly cross-reactive human monoclonal antibodies. J Virol 85: 13463-13467. doi: 10.1128/JVI.05193-11. PubMed: 21994454.
22. Blom AM (2004) Strategies developed by bacteria and virus for protection from the human complement system. Scand J Clin Lab Invest 64: 479-496. doi:10.1080/00365510410002904. PubMed: 15276914.
23. Finlay BB, McFadden G (2006) Anti-immunology: evasion of the host immune system by bacterial and viral pathogens. Cell 124: 767-782. doi:10.1016/j.cell.2006.01.034. PubMed: 16497587.
24. Avirutnan P, Hauhart RE, Somnuke P, Blom AM, Diamond MS et al. (2011) Binding of flavivirus nonstructural protein NS1 to C4b binding protein modulates complement activation. J Immunol 187: 424-433. doi: 10.4049/jimmunol.1100750. PubMed: 21642539.
25. Amet T, Ghabril M, Chalasani N, Byrd D, Hu N et al. (2012) CD59 incorporation protects hepatitis C virus against complement-mediated destruction. Hepatology 55: 354-363. doi:10.1002/hep.24686. PubMed: 21932413.
26. Banerjee A, Mazumdar B, Meyer K, Di Bisceglie AM, Ray RB et al. (2011) Transcriptional repression of C4 complement by hepatitis C virus proteins. J Virol 85: 4157-4166. doi:10.1128/JVI.02449-10. PubMed: 21345967.
27. Mazumdar B, Kim H, Meyer K, Bose SK, Di Bisceglie AM et al. (2012) Hepatitis C virus proteins inhibit C3 complement production. J Virol 86: 2221-2228. doi:10.1128/JVI.06577-11. PubMed: 22171262.
28. Kittlesen DJ, Chianese-Bullock KA, Yao ZQ, Braciale TJ, Hahn YS (2000) Interaction between complement receptor gC1qR and hepatitis C virus core protein inhibits T-lymphocyte proliferation. J Clin Invest 106: 1239-1249. doi:10.1172/JCI10323. PubMed: 11086025.

ELSEVIER

CrossMark

Institut Pasteur

Microbes and Infection 16 (2014) 114–122

www.elsevier.com/locate/micinf

Original article

Retinoids and rexinoids inhibit hepatitis C virus independently of retinoid receptor signaling

Yuko Murakami [a,*], Masayoshi Fukasawa [b], Yukihiro Kaneko [a], Tetsuro Suzuki [c], Takaji Wakita [d], Hidesuke Fukazawa [a,*]

[a] *Department of Chemotherapy and Mycoses, National Institute of Infectious Diseases, Tokyo 162-8640, Japan*
[b] *Department of Biochemistry and Cell Biology, National Institute of Infectious Diseases, Tokyo, Japan*
[c] *Department of Infectious Diseases, Hamamatsu University School of Medicine, Hamamatsu, Japan*
[d] *Department of Virology II, National Institute of Infectious Diseases, Tokyo, Japan*

Received 8 August 2013; accepted 21 October 2013
Available online 28 October 2013

Abstract

Using a high-throughput screening system involving HCV JFH-1-Huh 7.5.1 cells, we determined that the ligands of class II nuclear receptors, retinoids and rexinoids inhibit HCV infection. Retinoids, ligands of retinoic acid receptor (RAR), and rexinoids, ligands of retinoid X receptor (RXR), reduced extracellular HCV RNA of HCV infected cells in a dose-dependent manner. The 50% effective concentrations were below 10 nM, and the 50% cytotoxic concentrations were over 10 μM. Both agonists and antagonists demonstrated inhibition, which indicates that the effect is not dependent on retinoic acid signaling. These chemicals reduced HCV RNA and NS5A protein levels in cells harboring the sub-genomic HCV replicon RNA, which suggests that the chemicals affect HCV RNA replication. These compounds were also effective against persistently infected cells, although the reduction in the intracellular HCV RNA was smaller than that of the extracellular HCV RNA, suggesting that viral post-replication step is also inhibited. In combination with interferon (IFN), retinoid exhibited a synergistic effect. Retinoids did not enhance expression of the IFN effector molecule PKR. These series of compounds warrant further investigation as new class of HCV drugs, for the clinical translation of our observation may lead to increased anti-HCV efficacy.

Keywords: Hepatitis C virus; HCV; Retinoid; Retinoic acid; Rexinoid

1. Introduction

Hepatitis C virus (HCV) is a leading cause of chronic liver diseases such as hepatitis, cirrhosis, and hepatocellular carcinoma (HCC). HCC usually occurs after establishment of liver cirrhosis in HCV-infected individuals. Although the prevalence of HCV infection in HCC differs noticeably with geographical regions, two-thirds of hepatocellular carcinoma patients are chronically infected with HCV in Japan [1]. Because of limited efficacy and high cost of preexisting drugs, HCV infection has not yet been eradicated from the world especially Asia. The current standard therapy, a combination of interferon (IFN) and ribavirin, is not effective for all the patients, in addition to having serious side effects. Because of the urgent need for novel HCV therapies, many studies on HCV drugs have been conducted. In addition to *in vitro* screenings targeting specific HCV viral enzymes and screenings using HCV genome-harboring replicon cells, the HCV JFH-1-Huh 7.5 cell infection system has been recently developed [2] and is now used for screening. This system is applicable to easy screening assays [3,4] and is capable of identifying and analyzing inhibitors that have effects on any stages of HCV life cycle: viral attachment, entry, replication, and post-replication. This system targets not only viral components but also the host components involved in HCV infection.

* Corresponding authors. National Institute of Infectious Diseases, Toyama 1-23-1, Shinjuku-ku, Tokyo 162-8640, Japan. Tel.: +81 3 5285 1111x2327; fax: +81 3 5285 1272.
E-mail addresses: murakami@nih.go.jp (Y. Murakami), fukazawa@nih.go.jp (H. Fukazawa).

1286-4579/$ - see front matter © 2013 Institut Pasteur. Published by Elsevier Masson SAS. All rights reserved.
http://dx.doi.org/10.1016/j.micinf.2013.10.016

We screened chemical libraries using an easy high-throughput screening with the JFH-1-Huh 7.5 cell system [4], and discovered that several ligands of class II nuclear receptors inhibited HCV infection. These ligands had a notable effect on HCV infection; the 50% effective concentrations (EC_{50}) were below 10 nM. The nuclear receptors are classified into two classes: receptors for steroid hormones (class I) and receptors for non-steroid ligands (class II). The class II nuclear receptors include retinoic acid receptor (RAR), retinoid X receptor (RXR), peroxisome proliferator-activated receptors (PPARs), vitamin D receptor (VDR), thyroid hormone receptor (TR), and liver X receptor (LXR). The common biological characteristic of the class II receptors is that they work as a dimer with the RXR [5–7]. The RAR consists of three subtypes, α, β and γ, encoded by separate genes. All-*trans*-retinoic acid (ATRA) is a retinol (vitamin A) metabolite and considered as a natural ligand of RARs. ATRA and some synthetic analogs bind RARs and are referred to as retinoids [5,6]. ATRA is used as an effective anticancer drug for the treatment of acute promyelocytic leukemia (APL). Am80 is a synthetic retinoid with specific activation of RARα, which is also clinically used for APL as tamibarotene. RXR also consists of three subtypes, α, β, and γ. In addition, 9-*cis*-retinoic acid (9CRA) and some synthetic ligands of RXRs are called rexinoids [7]. RXR is unique in that it forms a homodimer, whereas all the other class II receptors exclusively form heterodimers with the RXR. 9CRA is also a metabolite of retinol and is believed to be a natural ligand of the RXR, but is capable of binding the RAR. Bexarotene is a synthetic selective agonist of RXR prescribed as Targretin and used for cutaneous T cell lymphomas in USA and some other countries.

There are some reports regarding the *in vitro* inhibitory effect on HCV of ATRA and other retinoids [8,9]. Furthermore, Böcher et al. reported a preclinical use of ATRA for the treatment of hepatitis C patients and demonstrated its therapeutic potential [10]. Nevertheless, the mechanism of the retinoid inhibitory effect on HCV has not been examined and remains unclear. Retinoids have been already approved for treatments of other diseases. That is, their pharmacological properties had been already investigated and safety is verified, suggesting benefit for HCV treatment. Therefore, in this study, we attempted to elucidate how retinoids and related chemicals inhibit HCV infection and obtain some clues allowing the understanding of the mechanism of action.

2. Materials and methods

2.1. Cells and virus

Huh 7.5.1 cells and 293T cells were cultured in Dulbecco's modified Eagle's medium (DMEM) (Sigma–Aldrich Co. St. Louis, MO, USA) with 10% fetal bovine serum (FBS). HCV JFH-1 (genotype 2a) (HCVcc) was generated and stocked as described previously [3]. Subgenomic replicon cells, clone #4-1 and clone #5-15, which are derived from Huh 7 cells, harbor the JFH-1 genome (genotype 2a) [11] and the genotype 1b HCV genome [12], respectively. A persistently infected cell line was prepared as described below. Huh 7 cells were inoculated with HCVcc at a multiplicity of infection (MOI) of 1. The cells were passaged every 3–5 days with a cell density at more than 5×10^5 cells/10 cm-dish. HCVcc inoculated cells were monitored via intracellular and extracellular HCV core protein levels as determined by ELISA (HCV ELISA Test System, Ortho-Clinical Diagnostic K. K., Tokyo, Japan) and immunostaining and immunoblot using a specific antibody (anti-HCV core protein antibody, #40015B, Anogen, Mississauga, Canada). After HCVcc inoculation of Huh 7 cells, the intracellular HCV RNA and extracellular infectivity were detected for over ten passages. These cells were also cultured in DMEM with FBS.

2.2. Chemicals

All-*trans*-retinoic acid (ATRA) was purchased from Calbiochem-Merck KGaA (Darmstadt, Germany) and 9-*cis*-retinoic acid (9CRA) was from LKT (St. Paul, MN, USA). Am80, adapalene, TTNTB, and GW3965 were purchased from Tocris Bioscience (Bristol, UK). LE135, bexarotene, CD3254, UVI3003, SR11237, and TO901317 were purchased from Sigma–Aldrich Co. Ro41-5253, GW1929, and vitamin D3 were purchased from Enzo Life Science Inc. (Farmingdale, NY, USA). Clofibrate was purchased from Cayman Chemicals (Ann Arbor, MI, USA), and thyroxin was from Santa Cruz Biotech Inc. (Santa Cruz, CA, USA). Human interferon (IFN) α was purchased from PeproTech Inc. (Princeton, NJ, USA).

2.3. Quantification of viral titer in the supernatant and cells

To detect the reduction of HCV RNA in the supernatant, we used an easy quantitative real-time RT-PCR, the tube-capture-RT-PCR described before [3]. Briefly, the test compounds were added to Huh 7.5.1 cells seeded in 96-well plates as was HCVcc (MOI = 0.01), and after 5 days, the culture supernatant was taken and subjected to quantitative real-time RT-PCR using the SuperScript III Platinum SYBR Green One-Step qRT-PCR Kit™ (Invitrogen Co., Carlsbad, CA, USA) by the Agilent Technologies Mx3000P (Santa Clara, CA, USA) [3]. For measuring the copy number of HCV RNA, 5×10^4 cells were seeded in 24-well plate per well, infected, and cultured for the indicated time. RNA was extracted with the QIAamp viral RNA Mini Kit™ (Qiagen GmbH, Hilden, Germany) from the supernatant or with the RNeasy Mini Kit ™ (Qiagen) from cells for quantitative real-time RT-PCR. The primers for HCV RNA were 5′-GAGT GTCGTACAGCCTCCAG-3′ (nucleotides 97–116) and 5′-AGGCCTTTCGCAACCCA-3′ (nucleotides 280–264). The standard JFH-1 RNA protocol for measurement of copy number has been previously described [3]. As an internal control, glyceraldehyde-3-phosphate-dehydrogenase (GAPDH) mRNA was measured with the primers 5′-CCACCCATGGCAAATTCC-3′ and 5′-TGGGATTTCCATTGAT-3′. To evaluate the expression of protein kinase R (PKR) and 2′, 5′-oligoadenylate synthetase 1 (OAS1), we used 5′-TGGCCGCTAAACTTGCATATC-3′ and 5′-GCGAGTGTGCTGGTCACTAAAG-3′ as primers for PKR